The Double-ICTZ Problem in IPCC AR4 Coupled GCMs: Ocean-Atmosphere Feedback Analysis

Jia-Lin Lin

NOAA ESRL/CIRES Climate Diagnostics Center, Boulder, CO

J. Climate, in press

Corresponding author address: Dr. Jia-Lin Lin
NOAA ESRL/CIRES Climate Diagnostics Center
325 Broadway, R/PSD1, Boulder, CO 80305-3328
Email: jialin.lin@noaa.gov
Web: http://www.cdc.noaa.gov/people/jialin.lin/

Abstract

This study examines the double-ITCZ (Intertropical Convergence Zone) problem in the coupled general circulation models (CGCMs) participating in the Inter-governmental Panel on Climate Change (IPCC) Fourth Assessment Report (AR4). The 20th century climate simulations of 22 IPCC AR4 CGCMs are analyzed, together with the available AMIP runs from 12 of them. To understand the physical mechanisms for the double-ITCZ problem, the main ocean-atmosphere feedbacks, including the zonal sea surface temperature (SST) gradient–trade wind feedback (or Bjerknes feedback), the SST–surface latent heat flux (LHF) feedback, and the SST–surface shortwave flux (SWF) feedback, are studied in detail.

The results show that most of the current state-of-the-art CGCMs have some degree of the double-ITCZ problem, which is characterized by excessive precipitation over much of the tropics (e.g. northern hemisphere ITCZ, South Pacific Convergence Zone, maritime continent, and equatorial Indian Ocean), and often associated with insufficient precipitation over equatorial Pacific. The excessive precipitation over much of the tropics usually causes overly strong trade winds, excessive LHF and insufficient SWF, leading to significant cold SST bias in much of the tropical oceans. Most of the models also simulate insufficient latitudinal asymmetry in precipitation and SST over eastern Pacific and Atlantic Oceans.

The AMIP runs also produce excessive precipitation over much of the tropics including equatorial Pacific, which also leads to overly strong trade winds, excessive LHF and insufficient SWF. This suggests that the excessive tropical precipitation is an intrinsic error of the atmospheric models, and that the insufficient equatorial Pacific

precipitation in the coupled runs of many models comes from ocean-atmosphere feedback. Feedback analysis demonstrates that the insufficient equatorial Pacific precipitation in different models is associated with one or more of the following three biases in ocean-atmosphere feedback over equatorial Pacific: (1) excessive Bjerknes feedback, which is caused by excessive sensitivity of precipitation to SST and overly strong time-mean surface wind speed; (2) overly positive SST-LHF feedback, which is caused by excessive sensitivity of surface air humidity to SST; and (3) insufficient SST-SWF feedback, which is caused by insufficient sensitivity of cloud amount to precipitation. Off the equator over the eastern Pacific stratus region, most of the models produce insufficient stratus-SST feedback associated with insufficient sensitivity of stratus cloud amount to SST, which may contribute to the insufficient latitudinal asymmetry of SST in their coupled runs. These results suggest that the double-ITCZ problem in CGCMs may be alleviated by reducing the excessive tropical precipitation and the above feedback-relevant errors in the atmospheric models.

1. Introduction

The tropical mean climate provides the background state for tropical variabilities such as the El Nino/Southern Oscillation (ENSO), the Madden-Julian Oscillation (MJO) and the convectively coupled equatorial waves, and modulates the spatial distribution of extreme weather events such as the tropical cyclones and mesoscale convective systems. It also provides the heating source for the Hadley circulation and affects the circulation patterns in the extratropics. Therefore, a good simulation of tropical mean climate by the climate models is a prerequisite for their good simulations/predictions of tropical variabilities and global teleconnections.

Unfortunately, the tropical mean climate has not been well simulated by the coupled general circulation models (CGCMs) used for climate predictions and projections (e.g. Neelin et al. 1992; Mechoso et al. 1995; Delecluse et al. 1998; Latif et al. 2001; Davey et al. 2002; Meehl et al. 2005). In particular, most of the CGCMs produce a double-ITCZ (Intertropical Convergence Zone) pattern with excessive precipitation off the equator but insufficient precipitation on the equator, which is often associated with an excessive and overly narrow sea surface temperature (SST) cold tongue that extends too far west into the western Pacific. This double-ITCZ problem is a long-standing tropical bias existing in the last several generations of CGCMs. Comparison between models with the double-ITCZ problem and those without the problem indicates that the problem is mainly caused by the atmospheric models rather than the ocean models (e.g. Schneider 2002). Sensitivity experiments with individual CGCMs also showed that the bias can be alleviated by modifying the atmospheric models, for example, by increasing the horizontal and vertical resolutions of the atmospheric model (e.g. Mechoso 2006),

changing the closure/trigger assumptions of convection scheme (e.g. Frey et al. 1997; Zhang and Wang 2006), or changing the surface wind stress formulation (e.g. Luo et al. 2004). However, as pointed out by Mechoso (2006), a synthetic view of the double-ITCZ problem is still elusive.

It is widely accepted that the ocean-atmosphere feedback plays a central role in determining the tropical mean climate. Many theories have been developed for the ocean-atmosphere feedback mechanisms in the coupled tropical mean climate system (e.g. Neelin and Dijkstra 1995; Dijkstra and Neelin 1995, 1999; Sun and Liu 1996; Jin 1996; Clement et al. 1996, 2005; Liu 1997; Liu and Huang 1997; Clement and Seager 1999; van der Vaart et al. 2000; Cai 2003). Related to this topic, the feedback mechanisms for regulating the warm pool SST have also been examined by many observational and modeling studies (e.g. Ramanathan and Collins 1991; Wallace 1992; Fu et al. 1992; Hartmann and Michelson 1993; Waliser and Graham 1993; Liu et al. 1994; Pierrehumbert 1995; Zhang et al. 1995; Miller 1997; Larson et al. 1999; Del Genio and Kovari 2002). Overall, the ocean-atmosphere feedbacks in the tropical mean climate system can be categorized into the following three groups (Figure 1):

(1) The SST gradient-trade wind feedback, or Bjerknes feedback (Bjerknes 1969; Neelin and Dijkstra 1995). The SST gradient between the warm pool and the cold tongue generates an east-west asymmetry in the atmospheric convection, precipitation, clouds and water vapor, leading to an east-west asymmetry in the total diabatic heating within the atmosphere, which is dominated by the latent heating associated with precipitation and the radiative heating associated with clouds and water vapor. The heating asymmetry forces sea level pressure (SLP) gradient and thus enhances the trade wind (the Walker

circulation). The increased trade wind in turn enhances the SST gradient by inducing thermocline depth gradient, vertical upwelling/downwelling, meridional Sverdrup transport, and zonal advection. Therefore, this Bjerknes feedback is a positive feedback.

(2) The SST-surface latent heat flux (LHF) feedback (e.g. Wallace 1992). Perturbation in SST affects the surface wind speed, surface air humidity, and sea-air humidity difference, and thus changes the surface LHF, while the LHF in turn modifies the SST. Previous observational studies have shown that the sign of the SST/LHF feedback is different for different geographical regions and different time scales (e.g. Liu et al. 1994; Zhang et al. 1995).

(3) The SST-surface shortwave flux (SWF) feedback (e.g. Ramanathan and Collins 1991). This feedback has different sign over the warm pool and the cold tongue. Over the warm pool, higher SST forces more active deep convection and more clouds, which in turn reduce the surface downward shortwave flux into the ocean and thus cools down the SST, leading to a negative feedback. Over the cold tongue, on the contrary, higher SST reduces the static stability of the boundary layer and thus reduces the low cloud amount (Klein and Hartmann 1993), which in turn increases the surface downward shortwave flux and warms up the SST, leading to a positive feedback.

Any positive (negative) feedback tends to enhance (weaken) the east-west gradient of SST and thus the Walker circulation, and the different feedbacks can enhance or counteract on each other. Moreover, theoretical studies (e.g. Neelin and Dijkstra 1995; Dijkstra and Neelin 1995) have shown that stronger positive feedback tends to shift the whole system more westward, leading to an excessive SST cold tongue/double-ITCZ pattern similar to that produced by many CGCMs. Moreover, ocean-atmosphere feedback

also affects the meridional asymmetry in central and eastern Pacific between the warm-SST/deep-convection region (ITCZ) north of the equator and the cold-SST/stratus region south of the equator (see review by Xie 2005). In particular, both the wind-evaporation-SST feedback (one form of the SST-LHF feedback; e.g. Xie and Philander 1994; Xie 1996a, Lin 2007) and the stratus-SST feedback (one form of the SST-SWF feedback; e.g. Philander et al. 1996; Ma et al. 1996; Yu and Mechoso 1999; Gordon et al. 2000; de Szoeke et al. 2006) enhance the meridional asymmetry associated with the continental forcing in the eastern boundary (e.g. Xie 1996a; Xie and Saito 2001), seasonal solar forcing (e.g. Xie 1996b), and atmosphere's internal dynamics (e.g. Charney 1971; Holton 1971; Lindzen 1974; Waliser and Somerville 1994; Chao 2000; Chao and Chen 2001, 2004; Liu and Xie 2002; Bacmeister et al. 2006; Chao et al. 2006). However, few previous studies have evaluated quantitatively the ocean-atmosphere feedback parameters in GCMs to understand the physical reasons of the double-ITCZ problem.

Recently, in preparation for the Inter-governmental Panel on Climate Change (IPCC) Fourth Assessment Report (AR4), more than 20 international climate modeling centers conducted a comprehensive set of long-term simulations for both the 20th century's climate and different climate change scenarios in the 21st century. Before conducting the extended simulations, many of the modeling centers applied an overhaul to their physical schemes to incorporate the state-of-the-art research results, and some also increased their model resolutions. These state-of-the-art climate models provide a valuable and exciting resource for studying the double-ITCZ problem because (1) they provide a wide range of model resolution and a large variety of model physics, such as all the major deep convection schemes with different types of convective closures, convective triggers, and

cloud models, making it possible to study the dependence of model performance on the basic model characteristics, and (2) more than half of the models also did AMIP runs in addition to the standard coupled runs, making it possible to trace the biases in the coupled runs back to the atmospheric models, and evaluate quantitatively the ocean-atmosphere feedback parameters important for the double-ITCZ problem.

The purpose of this study is to evaluate the tropical mean climate in 22 IPCC AR4 CGCMs, with an emphasis on the ocean-atmosphere feedback mechanisms for the double-ITCZ problem. The questions we address are:

(1) How well do the IPCC AR4 CGCMs simulate the tropical mean climate, especially the SST and precipitation? How well do the models simulate the surface momentum and heat fluxes?

(2) Is there any systematic dependence of model performance on the basic model characteristics, such as model resolution or model physics?

(3) Are the biases found in the coupled runs caused by the atmospheric models or by ocean-atmosphere coupling?

(4) How well do the atmospheric models simulate the ocean-atmosphere feedback parameters important for tropical mean climate?

The models and validation datasets used in this study are described in section 2. The CGCM simulations are evaluated in section 3. The AGCM simulations and feedback mechanisms are analyzed in section 4. A summary and discussion are given in section 5.

2. Models and validation datasets

This analysis is based on 20 years (model year 1979-1999) of the Climate of the 20th Century (20C3M) simulations from 22 CGCMs, together with the available AMIP runs (1979-1999) from 12 of them. Table 1 shows the model names and acronyms, their horizontal and vertical resolutions, brief descriptions of their deep convection schemes, and flux corrections. Models with same or similar deep convection schemes are listed together in Table 1 and in all the figures in this paper. For each model we use 20 years of monthly mean SST, precipitation, SLP, surface wind stress, surface downward shortwave flux (SWF), surface latent heat flux (LHF), and surface air specific humidity.

The model simulations are validated using multiple observational datasets (Table 2). For each variable, different datasets are used whenever possible in order to bracket the uncertainties associated with measurement/retrieval/analysis. Because we are interested only in the large-scale features, unless otherwise specified, all model outputs and observational datasets are averaged to have a zonal resolution of 10 degrees longitude but the original meridional resolutions are kept.

3. The double-ITCZ problem in the coupled runs

a. Precipitation and SST

Figure 2 shows the horizontal maps of annual mean SST (shading) and precipitation (contours) for observation and 22 IPCC AR4 CGCMs. For the convenience of presentation, the names used in this study for the different geographical regions are shown in Figure 2b. In observation (Figure 2a), most of the precipitation falls in the Indian Ocean, maritime continent, western equatorial Pacific, northern hemisphere ITCZ,

and southern hemisphere SPCZ (South Pacific Convergence Zone). The SPCZ tilts to the southeast, and the 5-mm/day contour stays to the west of 200E. The precipitation pattern does not follow the SST pattern very well. For example, precipitation is large over the eastern Pacific warm pool region where SST is about 27-28 C, but is small over southeastern Pacific (5S-15S, 200E-240E) where SST is also about 27-28 C, suggesting the existence of some physical processes suppressing deep convection over southeastern Pacific.

The observed precipitation/SST pattern is not well simulated by most of the models (Figure 2c-x). Of the 22 models, there are only four with heat flux correction (denoted by "adj" in Figure 2), and we will focus on the other 18 models without flux correction. Following Davey et al. (2002), we call these models "no-adj" models. The simulations of the "no-adj" models show three characteristics: (1) More than three-quarters of the models show a clear double-ITCZ pattern in precipitation, which is characterized by excessive precipitation over northern hemisphere ITCZ and southern hemisphere SPCZ, together with an incorrect east-west alignment of SPCZ with the 5 mm/day contour extending to the east of 200E. In most of the models there is also excessive precipitation over maritime continent and Indian Ocean, while in many models there is insufficient precipitation over equatorial Pacific (e.g. PCM, IAP, GISS-EH, HadGEM1, CNRM, BCCR, INM, and IPSL). (2) Models with double-ITCZ pattern in precipitation generally have an excessive SST cold tongue extending into the western Pacific (e.g. PCM, IAP, GISS-EH, HadGEM1, CNRM, BCCR, and INM), while those without double-ITCZ pattern often display realistic or overly warm SST along the equator (e.g. GISS-AOM, GISS-ER, and MIROC-hires). This suggests that the double-ITCZ problem is associated

with ocean-atmosphere feedback. (3) The precipitation pattern generally follows the SST pattern more closely in the models than in observation, especially over the southeastern Pacific (5S-15S, 200E-240E), suggesting that the convection schemes in the models are too sensitive to SST and do not capture well the physical processes suppressing deep convection, for example, over the southeastern Pacific.

To give a more quantitative evaluation of the SST and precipitation biases, we plot in Figure 3 and Figure 4 the zonal profiles of annual mean SST and precipitation, respectively. Figure 3 shows the zonal profiles of SST averaged between (a) 5N-15N, (b) 5N-5S, and (c) 5S-15S. There are two important things to note concerning Figure 3. First, strikingly, most of the models produce a significant cold SST bias (1 C or more in many cases) in much of the tropical oceans, not only along the equator as emphasized by many previous studies (e.g. Mechoso et al. 1995; Delecluse et al. 1998; Latif et al. 2001; Davey et al. 2002; Meehl et al. 2005), but also off the equator in both the northern and southern hemispheres. In other words, the extent of the SST cold tongue is excessive not only in the zonal direction as emphasized in previous studies, but also in the meridional direction. Furthermore, the zonal SST gradient in equatorial Pacific is overly small in most of the models (not shown). Second, most models produce a warm SST bias in the eastern Pacific stratus cloud region and the eastern Atlantic. The cold SST bias in western Atlantic and warm SST bias in eastern Atlantic make the zonal SST gradient in Atlantic Ocean opposite to that in observation, which is consistent with the results for earlier generations of CGCMs (e.g. Davey et al. 2002).

Figure 4 is same as Figure 3 but for precipitation. Figure 4 demonstrates two points. First, most of the models produce excessive precipitation over much of the tropics,

including Indian Ocean, maritime continent, ITCZ, SPCZ and eastern Atlantic, in spite of the significant cold SST bias in all these regions except eastern Atlantic. This suggests that deep convection in the models is not controlled solely by SST itself, but by some other processes such as SST gradient (e.g. Lindzen and Nigam 1987), moisture convergence, or surface heat fluxes. Similarly, although most of the models simulate insufficient precipitation over eastern Pacific warm pool, northwestern Atlantic and equatorial western Atlantic, which is consistent with the cold SST biases in those regions, this does not necessarily mean that deep convection is controlled by local SST in these regions. Other factors may also play some roles. Second, more than half of the models simulate insufficient precipitation over equatorial Pacific (Figure 4b; e.g. PCM, IAP, GISS-EH, HadGEM1, CSIRO, MPI, CNRM, BCCR, and INM), which is also a key feature of the double-ITCZ problem. As a result, the bias of zonal mean precipitation is much larger off the equator than on the equator (Figure 5).

The double-ITCZ problem also manifests in the latitudinal asymmetry of SST and precipitation. Figure 6 shows the interhemispheric difference (5N-15N average minus 5S-15S average) for annual mean (a) SST and (b) precipitation. Most of the models produce insufficient latitudinal SST asymmetry over eastern Pacific and Atlantic Oceans (Figure 6a), which is mainly caused by cold SST bias in the northern hemisphere (Figure 3a) and warm SST bias in the southern hemisphere (Figure 3c). Most of the models also simulate excessive latitudinal SST asymmetry near the western boundary of Pacific Ocean, which is mainly caused by cold SST bias in the southern hemisphere (Figure 3c). The model biases in precipitation asymmetry (Figure 6b) are generally consistent with those in SST asymmetry (Figure 6a), with most of the models simulating insufficient asymmetry over

eastern Pacific and Atlantic Oceans, but excessive asymmetry near the western boundary of Pacific Ocean.

Factors hypothesized to be important for tropical mean climate simulations include atmospheric model resolution, atmospheric model physics, and ocean model characteristics. We have two pairs of "no-adj" models with similar atmospheric models but in different resolution: CCSM3 (T85) vs PCM (T42), and MIROC-hires (T106) vs MIROC-medres (T42). CCSM3 does show better tropical mean climate than PCM, but MIROC-hires performs not as good as MIROC-medres. Therefore, increasing atmospheric model resolution does not always improve the simulation of tropical mean climate.

Regarding model physics, the 22 models provide a large variety of model physics, such as all the major deep convection schemes with different types of convective closures, convective triggers, and cloud models (Table 1). Models with same or similar deep convection schemes are listed together in Table 1 and in all the figures in this paper. All the "no-adj" models with Kuo-type convective closure/trigger (MPI, CNRM, and BCCR) have significant double-ITCZ problem. The only model with moist convective adjustment closure (INM) also has significant double-ITCZ problem. All other models have convection schemes that are similar to the Arakawa-Schubert (1974) scheme, but sometimes with a bulk cloud model instead of a spectral cloud model. Among these models, there is some hint that the ones with explicit moisture trigger tend to simulate better tropical mean climate (e.g. MIROC-medres, MIROC-hires, GFDL2.0, and GFDL2.1). We will come back to this point in the discussions in section 5.

Ocean model also plays an important role in simulating tropical mean climate. Evidence comes from comparison between GISS-ER and GISS-EH, which have identical atmospheric models but different ocean models (Dr. Anthony Del Genio, personal communication). They produce dramatically different mean climate, with double-ITCZ problem in GISS-EH but not in GISS-ER (e.g. Figure 2i and j). As will be shown by our feedback analysis in section 4b, the atmospheric model used by both GISS-EH and GISS-ER does produce some incorrect ocean-atmosphere feedback parameters which tend to cause insufficient equatorial Pacific precipitation. Therefore, it is likely that there are some processes in the GISS-ER ocean model that tend to cancel the atmospheric model errors.

In summary, most of the current state-of-the-art CGCMs have some degree of the double-ITCZ problem, which is characterized by excessive precipitation over much of the tropics (e.g. northern hemisphere ITCZ, southern hemisphere SPCZ, maritime continent, and equatorial Indian Ocean), and in many cases insufficient precipitation over equatorial Pacific. This is often associated with significant cold SST bias in much of the tropical oceans (both along and off the equator). Most of the models also simulate insufficient latitudinal asymmetry in SST and precipitation over eastern Pacific and Atlantic Oceans. We do not find any systematic dependence of model simulation on atmospheric model resolution, but do find some dependence on the choice of ocean model. There is also some hint that the models with explicit moisture trigger of deep convection tend to simulate better tropical mean climate.

b. Surface fluxes

To understand the cold SST biases in most of the models, we evaluate in this subsection the surface fluxes including surface wind stress, LHF, cloud amount, and SWF. Surface wind stress has been evaluated by some of the previous model intercomparison studies (e.g. Davey et al. 2002), but surface heat fluxes (LHF and SWF) have not been evaluated by previous intercomparison studies.

The excessive tropical precipitation (i.e. total latent heating) in most of the models significantly affects the surface zonal wind stress τ_x (Figure 7). Most of the models produce overly strong easterly τ_x (i.e. overly strong trade wind) over much of the tropical oceans, such as north Indian Ocean, ITCZ, eastern Pacific warm pool, equatorial Pacific, south Indian Ocean, and SPCZ. Most of the models also simulate overly strong westerly τ_x over maritime continent (near 100E) and eastern Atlantic, but overly weak easterly τ_x (i.e. overly weak trade wind) over western Atlantic. The distribution of τ_x bias is quite consistent with that of precipitation bias. For example, the overly strong easterly τ_x over equatorial Pacific and the overly strong westerly τ_x over maritime continent (Figure 7b) are consistent with the excessive heating near 120E in many models (Figure 4b), possibly through enhanced Walker circulation. The overly strong trade winds over equatorial Pacific, ITCZ and SPCZ are likely to enhance ocean upwelling and zonal advection, and thus contribute to the cold SST biases in those regions.

Besides directly forcing the ocean circulation, the surface wind biases also cause biases in LHF (Figure 8). The biases in LHF are quite consistent with the biases in τ_x (Figure 7), although the wind speed is also contributed by its meridional component. Most of the models produce excessive LHF over much of the tropical oceans, except over

the northwestern Atlantic and equatorial western Atlantic where the model surface winds are overly weak. Therefore, excessive LHF contributes to the cold SST bias in much of the tropical oceans.

In addition to LHF, another dominant term of surface heat flux is SWF, and it is expected that the significant biases in precipitation would lead to biases in cloud amount and thus SWF. The zonal profiles of total cloud amount are illustrated in Figure 9. Most of the models produce excessive cloud amount over maritime continent, ITCZ and SPCZ, but insufficient cloud amount over eastern Pacific warm pool, northwestern Atlantic, and equatorial western Atlantic, which is consistent with the sign of precipitation bias in those regions. However, over equatorial Pacific, many models with insufficient precipitation still produce nearly realistic or even excessive cloud amount, suggesting the presence of errors in the models' cloud fraction schemes. Consistent with the excessive cloud amount, most of the models simulate insufficient SWF over much of the tropical oceans (Figure 10), which contribute to the cold SST bias in those regions. Moreover, most of the models produce excessive SWF over the eastern Pacific stratus cloud region and eastern Atlantic, which contributes to the warm SST bias in those regions.

In short, the excessive precipitation over much of the tropics usually causes overly strong trade winds, excessive LHF, and insufficient SWF. These all contribute to the significant cold SST biases both along the equator and off the equator. Therefore, excessive tropical precipitation plays a central role in CGCM's tropical mean climate biases.

The double-ITCZ problem is a fairly generic problem and has been persisting in the last several generations of CGCMs in spite of the significant increase of model resolution

and continuous improvement of model physics. The major difficulty for understanding this problem is that it involves ocean-atmosphere feedback, i.e., the ocean drives the atmosphere and the atmosphere in turn also forces the ocean, which makes it difficult to determine the real cause of the final bias. One approach to overcome this difficulty is to evaluate separately each direction of the two-way interaction, for example, if the atmosphere model produces correct response when forced by observed SST (the AMIP run), and if the ocean model produces correct response when forced by observed surface fluxes. Fortunately, AMIP runs are available for 12 of the 22 IPCC AR4 GCMs. Therefore, in the next section we will evaluate the precipitation, surface fluxes, and ocean-atmosphere feedback parameters in the atmospheric models.

4. Atmospheric model biases important for ocean-atmosphere feedback

a. Precipitation and surface fluxes

Figure 11 shows the annual mean precipitation (contour) for the available AMIP runs of 12 models. Comparing with the coupled runs (Figure 2), the AMIP runs generally simulate more realistic annual mean precipitation pattern, with no model producing insufficient precipitation over equatorial Pacific. However, a closer look at the zonal profiles of precipitation (Figure 12) reveals that the AMIP runs also produce excessive precipitation over much of the tropics, not only off the equator but also along the equator. In particular, most of the models simulate excessive precipitation over equatorial Pacific (Figure 12b). Comparing Figure 12b with Figure 4b indicates that ocean-atmosphere coupling shifts the precipitation maximum westward in many models, causing the insufficient precipitation over equatorial Pacific (the physical mechanisms of which will

be analyzed in the next subsection). Therefore, excessive tropical precipitation is an intrinsic error of the atmospheric models. Ocean-atmosphere coupling, on the other hand, does not "cause" the excessive tropical precipitation, but only cause the insufficient equatorial Pacific precipitation in the coupled run of many models.

This point is further illustrated by the meridional profiles of zonal mean precipitation (Figure 13). The AMIP run of almost all models produces excessive precipitation throughout the tropics from 20S to 20N (Figure 13), with similar magnitude of bias on and off the equator. Comparison of Figure 13 with Figure 5 shows that ocean-atmosphere coupling acts to reduce the zonal mean precipitation near the equator (in addition to shifting the precipitation maximum westward) and enhances it off the equator.

The biases in latitudinal asymmetry of precipitation found in the coupled runs (Figure 6b) also exist in the AMIP runs (Figure 14). Most of the models produce insufficient asymmetry over eastern Pacific and Atlantic Oceans, but excessive asymmetry over Indian Ocean, maritime continent and western Pacific. This again supports our point that the precipitation bias is an intrinsic error of the atmospheric models, although it may be enhanced or migrated by ocean-atmosphere coupling in the coupled runs.

As can be expected, the excessive tropical precipitation in the AMIP runs leads to significant biases in surface wind stress and surface heat fluxes. Figure 15 shows an example along the equator. Most of the models produce overly strong trade winds over eastern Pacific (Figure 15a), possibly through enhanced Walker circulation, together with excessive LHF (Figure 15b), and often with insufficient SWF (Figure 15c). Therefore, most of the surface flux biases in the coupled runs already exist in the AMIP runs, but manifest themselves more in the coupled runs in the significant cold SST bias.

In summary, the AMIP runs also produce excessive precipitation over much of the tropics including equatorial Pacific, which also leads to overly strong trade winds, excessive LHF and insufficient SWF. This suggests that the excessive tropical precipitation is an intrinsic error of the atmospheric models, and that the insufficient equatorial Pacific precipitation in some coupled runs comes from ocean-atmosphere feedback. In the next subsection, we will evaluate directly the ocean-atmosphere feedback parameters to understand what causes the insufficient precipitation in equatorial Pacific.

b. Ocean-atmosphere feedback parameters

As discussed in the introduction, there are three major ocean-atmosphere feedbacks important for the coupled tropical mean climate system: (1) the SST gradient-trade wind (Bjerknes) feedback, (2) the SST-LHF feedback, and (3) the SST-SWF feedback. Any positive (negative) feedback tends to enhance (weaken) the east-west SST gradient and the Walker circulation. Moreover, theoretical studies (e.g. Dijkstra and Neelin 1995) have shown that stronger positive feedback tends to shift the whole system more westward, leading to an excessive SST cold tongue/double-ITCZ pattern similar to that produced by many CGCMs. However, the quantitative values of the ocean-atmosphere feedback parameters in GCMs have not been evaluated by previous model intercomparison studies.

The strength of the Bjerknes feedback can be measured by the linear regression coefficient of τ_x versus zonal SST gradient (Figure 16a). Several models generate overly strong τ_x for a given zonal SST gradient over equatorial Pacific, and thus produce an excessive Bjerknes feedback (e.g. MRI, MPI, CNRM, GISS-ER, and INM). The zonal

SST gradient first generates zonal precipitation (latent heating) gradient, and the zonal precipitation gradient in turn generates zonal SLP gradient (the zonal pressure gradient force), and then the zonal pressure gradient force drives τ_x. Many models produce excessive zonal precipitation gradient for a given zonal SST gradient especially near the dateline (Figure 16b), which will be shown shortly connected with excessive sensitivity of precipitation to SST in those models (cf. Figure 18b). Most of the models simulate quite realistic zonal pressure gradient for a given zonal precipitation gradient (Figure 16c), suggesting that the models produce quite good dynamical response to specified heating. However, a striking result is that almost all models produce overly strong τ_x for a given zonal pressure gradient force (Figure 16d). Does this suggest that all the models have insufficient mechanical damping in the boundary layer?

We plot in Figure 17a the linear regression of surface zonal wind (u) vs zonal pressure gradient force, which gives the reciprocal of the equivalent linear mechanical damping rate (Rayleigh damping rate). The observed value for both NCEP and ECMWF reanalysis is about 0.5-0.7 day, which is consistent with the result of Deser (1992) using COADS data. Most of the models produce quite realistic equivalent mechanical damping, especially near the date line. However, for a given value of u, most models produce an overly strong τ_x (Figure 17b), leading to the biases in Figure 16d. The bulk formula often used by both GCMs and observations to calculate τ_x is (e.g. Peixoto and Oort 1992):

$$\boldsymbol{\tau}_x = \rho\, C_D\, u\, |\mathbf{V}| \qquad (1)$$

where ρ is the surface air density, C_D the drag coefficient, and $\mathbf{V}$ the surface wind vector. When we regress τ_x against $u\,|\mathbf{V}|$ (Figure 17c), most of the models are quite consistent with one another and with both reanalyses, suggesting that they use similar value of C_D.

The overly large ratio between τ_x and u in most models (Figure 17b) is actually caused by the overly large time-mean surface wind speed $|\mathbf{V}|$ in those models (not shown, cf. Figure 15a). In other words, the bias in time-mean wind speed can contribute to bias in the Bjerknes feedback parameter through Eq. 1.

In many theoretical models, τ_x is not assumed to be related to SST gradient, but is assumed to be proportional to SST itself (see review by Neelin et al. 1998). Therefore, we also plot the linear regression coefficient of τ_x versus SST in Figure 18a. Again, several models produce overly strong τ_x for the same value of SST perturbation over equatorial Pacific (e.g. HadGEM1, MPI, CNRM, GISS-ER). All of these models also produce overly strong τ_x for the same value of SST gradient (Figure 16a), suggesting that their excessive Bjerknes feedback is quite robust independent of the choice of feedback parameters. These models tend to simulate excessive sensitivity of precipitation to SST (Figure 18b), which is connected to their excessive sensitivity of zonal precipitation gradient to zonal SST gradient (Figure 16b). They also tend to produce overly strong τ_x for a given value of precipitation (Figure 18c). This, again, is caused by the overly large ratio between τ_x and u in the models (Figure 17b) since most models actually simulate quite realistic u for a given value of precipitation (Figure 18d).

The strength of SST-LHF feedback can be measured by the linear regression of LHF versus SST (Figure 19a). In observation, the SST-LHF feedback is quite weak over much of the equatorial Pacific. In several models, however, LHF decreases significantly with SST increase, giving a strong positive feedback that tends to amplify any SST perturbation (e.g. CCSM3, PCM, GISS-ER, CNRM, and INM). LHF is affected by both surface wind speed and the difference between sea surface saturation specific humidity

(q_s) and surface air specific humidity (q_{air}). In observation, the surface wind speed (as represented here by the absolute value of τ) decrease with SST over equatorial Pacific (Figure 19b), which may be due to the surface wind convergence associated with enhanced convection. This is well captured by almost all models (Figure 19b). The observed q_s - q_{air} , on the other hand, increases with SST (Figure 19c), suggesting that when SST increases and q_s increases, q_{air} does not change as much as q_s. This is not well captured by the models, with many models producing insufficient increase of q_s - q_{air} with SST (Figure 19c; note q_{air} data is not available for four models), which in turn is caused by excessive sensitivity of q_{air} to SST (Figure 19d).

The strength of SST-SWF feedback can be measured by the linear regression of SWF versus SST (Figure 20a). In observation, SWF decreases with SST, and thus provides a negative feedback to SST that tends to damp any SST perturbation. Several models produce insufficient SST-SWF feedback over equatorial Pacific (e.g. MIROC-medres, MIROC-hires, and PCM), while several other models simulate excessive SST-SWF feedback (e.g. MPI, CNRM, IPSL, INM, CCSM3 and MRI). The SST-SWF feedback loop is as follows: increase of SST enhances precipitation, while precipitation in turn increases cloud amount, and cloud reduces the SWF. We have known that most of the models tend to produce excessive sensitivity of precipitation to SST (Figure 16c), which tends to cause excessive SST-SWF feedback. Then, what causes the insufficient SST-SWF feedback in several models? Actually, it is mainly caused by *insufficient sensitivity of cloud amount to precipitation in almost all models* (Figure 20b), which leads to insufficient sensitivity of cloud to SST (Figure 20c). Another contributing factor in one or two models is insufficient reduction of SWF associated with increased cloud amount

(Figure 20d; e.g. PCM), which may be associated with too-small cloud optical depth in those models.

Besides the effects on the east-west asymmetry along the equator, ocean-atmosphere feedback also plays an important role in maintaining the north-south asymmetry in tropical Pacific. There are two major ocean-atmosphere feedback mechanisms: the wind-evaporation-SST feedback (one form of the SST-LHF feedback; e.g. Xie and Philander 1994) and the stratus-SST feedback (one form of the SST-SWF feedback; e.g. Philander et al. 1996). The strength of wind-evaporation-SST feedback can be measured by the linear regression of interhemispheric LHF difference (ΔLHF) versus interhemispheric SST difference ((ΔSST; Figure 21a). In observation, ΔLHF decreases with ΔSST increase over much of the Pacific Ocean, and thus enhances ΔSST and provides a positive feedback. Several models produce overly strong feedback (e.g. CCSM3, PCM, MIROC-hires), which is caused by excessive sensitivity of LHF to ΔSST in both the northern hemisphere (Figure 21b) and the southern hemisphere (Figure 21c). One model (MRI) simulates overly weak wind-evaporation-SST feedback which is associated with insensitivity of LHF to ΔSST in both hemispheres.

The strength of stratus-SST feedback can be measured by the linear regression of SWF versus SST in the southern hemisphere stratus region (260E-280E; Figure 22a). In observation, SWF increases with SST, which provides a positive feedback and enhances the meridional SST asymmetry. Most of the models simulate too-weak stratus-SST feedback, which is caused by the insufficient sensitivity of stratus cloud amount to SST in those models (Figure 22b). This may contribute to the warm SST bias in the stratus

region in their coupled runs (Figure 3c), and the associated insufficient latitudinal SST asymmetry (Figure 6a).

To summarize, feedback analysis demonstrates that the insufficient equatorial Pacific precipitation in different models is associated with one or more of the following three biases in ocean-atmosphere feedback over equatorial Pacific: (1) excessive Bjerknes feedback, which is caused by excessive sensitivity of precipitation to SST and overly strong time-mean surface wind speed; (2) overly positive SST-LHF feedback, which is caused by excessive sensitivity of surface air humidity to SST; and (3) insufficient SST-SWF feedback, which is caused by insufficient sensitivity of cloud amount to precipitation. Off the equator only a few models simulate unrealistic wind-evaporation-SST feedback. However, over the eastern Pacific stratus region, most of the models produce insufficient stratus-SST feedback associated with insufficient sensitivity of stratus cloud amount to SST, which may contribute to the insufficient latitudinal SST asymmetry in their coupled runs.

For a certain model, the biases in different feedbacks may enhance or cancel each other. For example, the overly positive SST-LHF feedback in CCSM3 is largely cancelled by the excessive negative SST-SWF feedback, i.e., the total surface heat flux response to SST is nearly correct. Similar cancellation also occurs for the MIROC-medres model. On the contrary, in several other models (e.g. PCM, CNRM), biases in different feedbacks enhance each other, which may contribute to their significantly insufficient precipitation over equatorial Pacific.

The errors in the atmospheric models may also be enhanced or cancelled by those in the ocean models. The ocean model is highly involved in the Bjerknes feedback through

the wind-driven ocean circulation, and is also involved in the SST-LHF feedback and the SST-SWF feedback through the ocean mixed layer heat budget. For example, although the atmospheric model of GISS-ER produces excessive Bjerknes feedback and overly positive SST-LHF feedback, when coupled to different ocean models, the biases only manifest in GISS-EH but not in GISS-ER, suggesting that the GISS-ER ocean model has some processes that cancel the atmospheric model errors. On the other hand, for the IAP model, we do not find any significant error in the feedback parameters in its atmospheric model, but its coupled run displays insufficient equatorial Pacific precipitation, suggesting that its ocean model may produce some incorrect feedback.

5. Summary and discussion

This study examines the double-ITCZ problem in the IPCC AR4 CGCMs. The 20th century climate simulations of 22 IPCC AR4 CGCMs are analyzed, together with the available AMIP runs from 12 of them. To understand the physical mechanisms for the double-ITCZ problem, the main ocean-atmosphere feedbacks, including the Bjerknes feedback, the SST-LHF feedback, and the SST-SWF feedback, are studied in detail.

The results show that most of the current state-of-the-art CGCMs have some degree of the double-ITCZ problem, which is characterized by excessive precipitation over much of the tropics (e.g. northern hemisphere ITCZ, southern hemisphere SPCZ, maritime continent, and equatorial Indian Ocean), and often associated with insufficient precipitation over equatorial Pacific. The excessive precipitation over much of the tropics usually causes overly strong trade winds, excessive LHF and insufficient SWF, leading to significant cold SST bias in much of the tropical oceans. Most of the models also

simulate insufficient latitudinal asymmetry in precipitation and SST over eastern Pacific and Atlantic Oceans.

The AMIP runs also produce excessive precipitation over much of the tropics including equatorial Pacific, which also leads to overly strong trade winds, excessive LHF and insufficient SWF. This suggests that the excessive tropical precipitation is an intrinsic error of the atmospheric models, and that the insufficient equatorial Pacific precipitation in the coupled runs of many models comes from ocean-atmosphere feedback. Feedback analysis demonstrates that the insufficient equatorial Pacific precipitation in different models is associated with one or more of the following three biases in ocean-atmosphere feedback: (1) excessive Bjerknes feedback, which is caused by excessive sensitivity of precipitation to SST and overly strong time-mean surface wind speed; (2) overly positive SST-LHF feedback, which is caused by excessive sensitivity of surface air humidity to SST; and (3) insufficient SST-SWF feedback, which is caused by insufficient sensitivity of cloud amount to precipitation. Off the equator most of the models simulate realistic or excessive wind-evaporation-SST feedback. However, over the eastern Pacific stratus region, most of the models produce insufficient stratus-SST feedback associated with insufficient sensitivity of stratus cloud amount to SST, which may contribute to the insufficient meridional asymmetry of SST in their coupled runs. These results suggest that the double-ITCZ problem in CGCMs may be alleviated by reducing the excessive tropical precipitation and the above feedback-relevant errors in the atmospheric models. Figure 23 summarizes schematically the tropical mean climate biases in many IPCC AR4 CGCMs and the AGCM biases in ocean-atmosphere feedback parameters.

Overall, our results reveal five common biases in many climate models, namely

(1) excessive tropical precipitation,

(2) excessive sensitivity of precipitation to SST,

(3) excessive sensitivity of surface air humidity to SST,

(4) insufficient sensitivity of cloud amount to precipitation, and

(5) insufficient sensitivity of stratus cloud amount to SST.

The first three biases are all connected in some way to deep convection, and are consistent with another bias in the IPCC AR4 models identified by Lin et al. (2006a) – the too-strong persistence of tropical precipitation. A possible way to alleviate these biases is to include some observed negative feedback mechanisms to the deep convection schemes to suppress the deep convection, decouple the deep convection from SST, and to some extent decouple the boundary layer from SST. The observed negative feedback processes in deep convection include: (1) control of deep convection by lower troposphere moisture (e.g. Brown and Zhang 1997); (2) drying and cooling of the boundary layer by convective downdrafts, especially unsaturated convective downdrafts (e.g. Zipser 1969, Houze 1977, Barnes and Garstang 1982), and (3) drying of the lower troposphere by mesoscale downdrafts (e.g. Zipser 1969, 1977; Houze 1977, 1982; Mapes and Houze 1995; Mapes and Lin 2005). The current GCMs have not included all the above negative feedback processes in deep convection (Table 1). Although many of the models have saturated convective downdrafts, only one of them has unsaturated convective downdrafts (IPSL using the Emanuel 1991 convection scheme), and none of the models has mesoscale downdrafts. Moreover, the control of deep convection by lower troposphere moisture has not been well represented in many models, especially because

they include undiluted or weakly diluted updrafts in the cloud model. Only several models have included some form of moisture trigger (e.g. MIROC-medres, MIROC-hires, GFDL2.0, GFDL2.1), and our results suggest that these models tend to simulate better tropical mean climate.

Our analysis mainly focuses on the atmospheric model errors important for the double-ITCZ problem, but the ocean model also plays an important role in ocean-atmosphere feedbacks, especially in the Bjerknes feedback. Unfortunately, ocean model experiments forced by observed surface momentum and heat fluxes (the "OMIP" runs) are not available for the IPCC AR4 models, and in the future we will try to analyze the OMIP runs from some individual models to further understand the role of ocean models in the double-ITCZ problem.

Acknowledgements

This study benefited much from discussions with Brian Mapes, Chris Bretherton, Ed Schneider, and Winston Chao. It also benefited from the careful and insightful reviews of Shang-Ping Xie and two anonymous reviewers. This work was supported by the U.S. CLIVAR CMEP Project, NOAA CPO/CVP Program, NOAA CPO/CDEP Program, and NASA MAP Program. The ISCCP surface flux data were obtained from the OAFLUX website. The TRMM data were acquired as part of the Tropical Rainfall Measuring Mission (TRMM). The algorithms were developed by the TRMM Science Team. The data were processed by the TRMM Science Data and Information System (TSDIS) and the TRMM Office; they are archived and distributed by the Goddard Distributed Active Archive Center.

REFERENCES

Adler, R.F., G.J. Huffman, A. Chang, R. Ferraro, P. Xie, J. Janowiak, B. Rudolf, U. Schneider, S. Curtis, D. Bolvin, A. Gruber, J. Susskind, and P. Arkin, 2003: The Version 2 Global Precipitation Climatology Project (GPCP) Monthly Precipitation Analysis (1979-Present). J. Hydrometeor., 4,1147-1167.

Arakawa, A., and W. H. Schubert, 1974: Interaction of a Cumulus Cloud Ensemble with the Large-Scale Environment, Part I. *J. Atmos. Sci*., 31, 674–701.

Bacmeister, J. T., M. J. Suarez, and F. R. Robertson, 2006: Rain Reevaporation, Boundary Layer–Convection Interactions, and Pacific Rainfall Patterns in an AGCM. J. Atmos. Sci., 62, 3383-3403.

Barnes, G. M., and M. Garstang. 1982: Subcloud Layer Energetics of Precipitating Convection. *Mon. Wea. Rev.*, **110**, 102–117.

Betts, A. K., 1986: A new convective adjustment scheme. Part I: Observational and theoretical basis. *Quart. J. Roy. Meteor. Soc.,* **112,** 677–691.

Bjerknes, J., 1969: Atmospheric teleconnections from the equatorial Pacific, *Mon. Weather Rev*., *97*, 163–172.

Bougeault, P., 1985: A Simple Parameterization of the Large-Scale Effects of Cumulus Convection. *Monthly Weather Review*, 113, 2108–2121.

Brown, R. G., and C. Zhang, 1997: Variability of midtropospheric humidity and its effect on cloud-top height distribution during TOGA COARE. *J. Atmos. Sci.,* **54,** 2760-2774.

Cai, M., 2003: Formation of the Cold Tongue and ENSO in the Equatorial Pacific Basin. *Journal of Climate*: Vol. 16, No. 1, pp. 144–155.

Chao, W. C., 2000: Multiple equilibria of the ITCZ and the origin of monsoon onset. *J. Atmos. Sci.*, **57**, 641-652.

Chao, W. C., and B. Chen, 2001: Multiple equilibria of the ITCZ and the origin of monsoon onset. Part II: Rotational ITCZ attractors. *J. Atmos. Sci.*, **58**, 2820-2831.

Chao, W. C., and B. Chen, 2004: Single and double ITCZ in an Aqua-Planet model with constant SST and solar angle. *Climate Dynamics*, **22**, 447-459.

Chao, W. C., M. J. Suarez, J. T. Bacmeister, B. Chen, and L. Takacs, 2006: The Origin of systematic errors in the GCM simulation of ITCZ precipitation over oceans. J. Atmos. Sci., submitted.

Charney, J. G. 1971: Tropical cyclogenesis and the formation of the intertropical convergence zone. In, Reid, W.H. (ed.). *Mathematical Problems of Geophysical Fluid Dynamics.* Providence, Rhode Island: American Mathematics Society.

Clement, A. C., and R. Seager, 1999: Climate and the tropical oceans. *J. Climate.,* **12**, 3384–3401.

Clement, A. C., R. Seager, M. A. Cane, and S. E. Zebiak, 1996: An ocean dynamical thermostat. *J. Climate.,* **9**, 2190–2196.

Clement, A. C., R. Seager, and R. Murtugudde. 2005: Why Are There Tropical Warm Pools? *J. Climate*, 18, 5294–5311.

Davey, M. K., and coauthors, 2002: STOIC: a study of coupled model climatology and variability in tropical ocean regions, *Clim. Dyn., 18*, 403–420.

de Szoeke, S.P., Y. Wang, S.-P. Xie, and T. Miyama, 2006: The effect of shallow cumulus convection on the eastern Pacific climate in a coupled model. *Geophys. Res. Lett*., 33, L17713, doi: 10.1029/2006GL026715.

Del Genio, A. D., and M.-S. Yao, 1993: Efficient cumulus parameterization for long-term climate studies: The GISS scheme. *The Representation of Cumulus Convection in Numerical Models, Meteor. Monogr.,* No. 46, Amer. Meteor. Soc., 181–184.

Del Genio, A. D., and W. Kovari, 2002: Climatic properties of tropical precipitating convection under varying environmental conditions. *J. Climate.,* **15**, 2597–2615.

Delecluse, P., M. Davey, Y. Kitamura, S. Philander, M. Suarez, and L. Bengtsson, 1998: Coupled general circulation modeling of the tropical Pacific. *J. Geophys. Res.,* **103**, 14357–14373.

Deser, C., 1992: Diagnosis of the surface momentum balance over the tropical Pacific Ocean. *J. Climate,* 6, 64-74.

Dijkstra, H. A., and J. D. Neelin, 1995: Ocean–atmosphere interaction and the tropical climatology. Part II: Why the Pacific cold tongue is in the east. *J. Climate.,* **8**, 1343–1359.

Dijkstra, H. A., and J. D. Neelin, 1999: Coupled process and the tropical climatology. Part III: Instabilities of the fully coupled climatology. *J. Climate.,* **12**, 1630–1643.

Emanuel, K. A., 1991: A Scheme for Representing Cumulus Convection in Large-Scale Models. *Journal of the Atmospheric Sciences*, 48, 2313–2329.

Emori, S., T. Nozawa, A. Numaguti and I. Uno (2001): Importance of cumulus parameterization for precipitation simulation over East Asia in June, J. Meteorol. Soc. Japan, 79, 939-947.

Frey, H., M. Latif and T. Stockdale. 1997: The Coupled GCM ECHO-2. Part I: The Tropical Pacific. *Monthly Weather Review*: Vol. 125, No. 5, pp. 703–720.

Fu, R., A. D. DelGenio, W. B. Rossow, and W. T. Liu, 1992: Cirrus cloud thermostat for tropical sea surface temperatures tested using satellite data. *Nature.,* **358**, 394–397.

Gibson, J. K., P. Kållberg, S. Uppala, A. Hernandez, A. Nomura, and E. Serrano, 1997: ERA description. ECMWF Reanalysis Project Report Series 1, 86 pp.

Gordon, C.T., A. Rosati, and R. Gudgel. 2000. Tropical sensitivity of a coupled model to specified ISCCP low clouds. *Journal of Climate* 13: 2239–2260.

Gregory, D., and P. R. Rowntree. 1990: A Mass Flux Convection Scheme with Representation of Cloud Ensemble Characteristics and Stability-Dependent Closure. *Mon. Wea. Rev*., 118, 1483–1506.

Hartmann, D. L., and M. L. Michelsen, 1993: Large-scale effects on the regulation of tropical sea surface temperature. *J. Climate.,* **6**, 2049–2062.

Holton, J. R., J.M. Wallace, and J.A. Young, 1971: On Boundary Layer Dynamics and the ITCZ. *J. Atmos. Sci.*, **28**, 275-280.

Houze, R. A., 1977: Structure and Dynamics of a Tropical Squall–Line System. *Monthly Weather Review*, 105, 1540–1567.

Houze, R. A., 1982: Cloud clusters and large-scale vertical motions in the Tropics. *J. Meteor. Soc. Japan*, **60**, 396-410.

Jin, F.-F., 1996: Tropical ocean–atmosphere interaction, the Pacific cold tongue, and the El Niño/Southern Oscillation. *Science.,* **274**, 76–78.

Kalnay, E., and Coauthors, 1996: The NCEP/NCAR 40-Year Reanalysis Project. *Bull. Amer. Meteor. Soc.,* **77,** 437–471.

Klein, S. A., and D. L. Hartmann. 1993: The Seasonal Cycle of Low Stratiform Clouds. *J. Climate*, 6, 1587–1606.

Larson, K., D. L. Hartmann, and S. A. Klein, 1999: On the role of clouds, water vapor, circulation, and boundary layer structure on the sensitivity of the tropical climate. *J. Climate.,* **12**, 2359–2374.

Latif, M., and coauthors, 2001: ENSIP: the El Niño simulation intercomparison project, *Clim. Dyn., 18*, 255–276.

Lin, J. L., 2007: The wind-evaporation-SST feedback mechanism for latitudinal asymmetry of the ITCZ: Observational evidence. *Geophys. Res. Lett*, to be submitted.

Lin, J. L., G.N. Kiladis, B.E. Mapes, K.M. Weickmann, K.R. Sperber, W.Y. Lin, M. Wheeler, S.D. Schubert, A. Del Genio, L.J. Donner, S. Emori, J.-F. Gueremy, F. Hourdin, P.J. Rasch, E. Roeckner, and J.F. Scinocca, 2006a: Tropical intraseasonal variability in 14 IPCC AR4 climate models. Part I: Convective signals. *J. Climate*, **19**, 2665-2690.

Lin, J. L., B. E. Mapes, and W. Han, 2006b: What are the sources of mechanical damping in Matsuno-Gill type models? *J. Climate*, in revision.

Lindzen, R. S., 1974: Wave-CISK in the tropics. *J. Atmos. Sci.*, 31, 156-179.

Lindzen, R. S., and S. Nigam. 1987: On the Role of Sea Surface Temperature Gradients in Forcing Low-Level Winds and Convergence in the Tropics. *J. Atmos. Sci.*, 44, 2418–2436.

Liu, W.T. and X. Xie, 2002: Double Intertropical Convergence Zoens ñ a new look using scatterometer. *Geophys. Res. Lett*., 29(22), 2072, doi:10.1029/2002GL015431.

Liu, W.T., A. Zheng, and J. Bishop, 1994: Evaporation and solar irradiance as regulators of the seasonal and internanual variabilities of sea surface temperature, *J. Geophys. Res.*, 99, 12623-12637.

Liu, Z., 1997: Oceanic regulation of the atmospheric Walker circulation. *Bull. Amer. Meteor. Soc.,* **78**, 407–411.

Liu, Z., and B. Huang, 1997: A coupled theory of the tropical climatology: Warm pool, cold tongue, and Walker circulation. *J. Climate.,* **10**, 1662–1679.

Luo, J. J., S. Masson, E. Roeckner, G. Madec and T. Yamagata. 2005: Reducing Climatology Bias in an Ocean–Atmosphere CGCM with Improved Coupling Physics. *Journal of Climate*: Vol. 18, No. 13, pp. 2344–2360.

Ma, C.-C., C. R. Mechoso, A. W. Robertson, and A. Arakawa, 1996: Peruvian stratus clouds and the tropical Pacific circulation: A coupled ocean–atmosphere GCM study. *J. Climate.,* **9**, 1635–1645.

Mapes, B. E., and R. A. Houze, 1995: Diabatic divergence profiles in western Pacific mesoscale convective systems. *J. Atmos. Sci.*, **52**, 1807-1828.

Mapes, B. E., and J. L. Lin, 2005: Doppler radar observations of mesoscale wind divergence in regions of tropical convection. *Mon. Wea. Rev*., 133, 1808-1824.

Mechoso, C. R., 2006: Modeling the south eastern Pacific climate: Progress and challenges. NCEP EMC seminar. Powerpoint file available at:
http://www.emc.ncep.noaa.gov/seminars/presentations/2006/Mechoso.NCEP.Jan.06.ppt

Mechoso, C. R., and Coauthors, 1995: The seasonal cycle over the tropical Pacific in coupled ocean–atmosphere general circulation models. *Mon. Wea. Rev.,* **123**, 2825–2838.

Meehl, G. A., C. Covey, B. McAvaney, M. Latif and R. J. Stouffer. 2005: OVERVIEW OF THE COUPLED MODEL INTERCOMPARISON PROJECT. *Bulletin of the American Meteorological Society*, 86, 89–93.

Miller, R. L., 1997: Tropical thermostats and low cloud cover. *J. Climate.,* **10**, 409–440.

Moorthi, S., and Suarez M. J., 1992: Relaxed Arakawa–Schubert: A parameterization of moist convection for general circulation models. *Mon. Wea. Rev.,* **120**, 978–1002.

Neelin, J. D., and H. A. Dijkstra, 1995: Ocean–atmosphere interaction and the tropical climatology. Part I: The dangers of flux-correction. *J. Climate.,* **8**, 1325–1342.

Neelin, J. D., and Coauthors,, 1992: Tropical air–sea interaction in general circulation models. *Climate Dyn.,* **7**, 73–104.

Neelin, J. D., D. S. Battisti, A. C. Hirst, F-F. Jin, Y. Wakata, T. Yamagata, and S. E. Zebiak, 1998: ENSO theory, *J. Geophys. Res*., *103*, 14,262–14,290.

Nordeng, T.E., 1994: Extended versions of the convective parameterization scheme at ECMWF and their impact on the mean and transient activity of the model in the tropics. Technical Memorandum No. 206, European Centre for Medium-Range Weather Forecasts, Reading, United Kingdom.

Pan, D.-M., and D. A. Randall (1998), A cumulus parameterization with a prognostic closure, *Q. J. R. Meteorol. Soc*., 124, 949-981.

Peixoto, J. P., and A. H. Oort, 1992: *Physics of Climate*. American Institute of Physics, 520pp.

Philander, S. G. H., D. Gu, D. Halpern, G. Lambert, N.-C. Lau, T. Li, and R. C. Pacanowski,1996: Why the ITCZ is mostly north of the equator. *J. Climate,* 9, 2958–2972.

Pierrehumbert, R. T., 1995: Thermostats, radiator fins, and the runaway greenhouse. *J. Atmos. Sci.,* **52**, 1784–1806.

Ramanathan, V., and W. Collins, 1991: Thermodynamic regulation of ocean warming by cirrus clouds deduced from observations of the 1987 El Niño. *Nature.,* **351**, 27–32.

Rayner, N. A.; Parker, D. E.; Horton, E. B.; Folland, C. K.; Alexander, L. V.; Rowell, D. P.; Kent, E. C.; Kaplan, A., 2003: Global analyses of sea surface temperature, sea ice, and night marine air temperature since the late nineteenth century J. Geophys. Res., 108, No. D14, 4407 10.1029/2002JD002670.

Rossow, W.B., A.W. Walker, D.E. Beuschel, and M.D. Roiter, 1996: International Satellite Cloud Climatology Project (ISCCP) Documentation of New Cloud Datasets. WMO/TD-No. 737, World Meteorological Organization, 115 pp.

Russell GL, Miller JR, Rind D, 1995. A coupled atmosphere-ocean model for transient climate change studies. Atmosphere-Ocean 33 (4), 683-730.

Schneider, E. K., 2002: Understanding Differences between the Equatorial Pacific as Simulated by Two Coupled GCMs. *J. Climate*, 15, 449–469.

Smith, T.M., and R.W. Reynolds, 2004: Improved Extended Reconstruction of SST (1854-1997). *J. Climate*, 17, 2466-2477.

Sun, D.-Z., and Z. Liu, 1996: Dynamic ocean–atmosphere coupling: A thermostat for the tropics. *Science.,* **272**, 1148–1150.

Tiedke, M., 1989: A comprehensive mass flux scheme for cumulus parameterization in large-scale models. *Mon. Wea. Rev.,* **117**, 1779-1800.

Tokioka, T., K. Yamazaki, A. Kitoh, and T. Ose, 1988: The equatorial 30-60-day oscillation and the Arakawa-Schubert penetrative cumulus parameterization. *J. Meteor. Soc. Japan*, **66**, 883-901.

van der Vaart, P. C. F., H. A. Dijkstra, and F.-F. Jin, 2000: The Pacific cold tongue and the ENSO mode: A unified theory within the Zebiak–Cane model. *J. Atmos. Sci.,* **57**, 967–988.

Waliser, D. E., and N. E. Graham, 1993: Convective cloud systems and warm-pool sea-surface temperatures—Coupled interactions and self-regulation. *J. Geophys. Res.,* **98D**, 12881–12893.

Waliser, D. E., and R. C. J. Somerville, 1994: The preferred latitudes of the intertropical convergence zone. Journal of the Atmospheric Sciences, 51, 1619-1639.

Wallace, J. M., 1992: Effect of deep convection on the regulation of tropical sea surface temperature. *Nature.,* **357**, 230–231.

Xie, S.-P, 1996a: Westward propagation of latitudinal asymmetry in a coupled ocean-atmosphere model. *Journal of Atmospheric Science,* 53, 3236–3250.

Xie, S.-P., 1996b: Effects of seasonal solar forcing on latitudinal asymmetry of the ITCZ. J. Climate, 9, 2945-2950.

Xie, S.-P, 2005: The shape of continents, air-sea interaction, and the rising branch of the Hadley Circulation. In H.F. Diaz and R.S. Bradley (eds.), The Hadley Circulation: Present, Past and Future, 121–152. Kluwer Academic Publishers.

Xie, S.-P., and S. G. H. Philander. 1994. A coupled ocean-atmosphere model of relevance to the ITCZ in the eastern Pacific. *Tellus* 46A, 340–350.

Xie, S.-P. and K. Saito, 2001: Formation and variability of a northerly ITCZ in a hybrid coupled AGCM: Continental forcing and ocean-atmospheric feedback. *J. Climate*, 14, 1262-1276.

Yu, J.-Y., and C. R. Mechoso, 1999: Links between annual variations of Peruvian stratocumulus clouds and of SST in the eastern equatorial Pacific. *J. Climate,* 12, 3305–3318.

Zhang, G. J. and N. A. McFarlane, 1995: Sensitivity of climate simulations to the parameterization of cumulus convection in the CCC-GCM. *Atmos.-Ocean*, **3**, 407-446.

Zhang, G. J., and H. Wang, 2006: Toward mitigating the double ITCZ problem in NCAR CCSM3. *Geophys. Res. Lett.,* **33,** L06709 , doi:10.1029/2005GL025229.

Zhang, G. J., V. Ramanathan, and M. J. McPhaden, 1995: Convection–evaporation feedback in the equatorial Pacific. *J. Climate.,* **8**, 3040–3051.

Zhang, Y-C., W.B. Rossow, A.A. Lacis, V. Oinas, and M.I. Mishchenko, 2004: Calculation of radiative fluxes from the surface to top of atmosphere based on ISCCP and other global data sets: Refinements of the radiative transfer model and the input data. *J. Geophys. Res.*, 109, D19105, doi:10.1029/2003JD004457.

Zipser, E. J., 1969: The Role of Organized Unsaturated Convective Downdrafts in the Structure and Rapid Decay of an Equatorial Disturbance. *J. Appl. Meteor.*, **8**, 799–814.

Zipser, E. J., 1977: Mesoscale and Convective–Scale Downdrafts as Distinct Components of Squall-Line Structure. *Mon. Wea. Rev.*, 105, 1568–1589.

FIGURE CAPTIONS

Figure 1. Schematic depiction of the ocean-atmosphere feedback mechanisms in tropical mean climate system.

Figure 2. Annual mean SST (shading) and precipitation (contour) for observation and 22 IPCC AR4 CGCMs. Contour starts at 5 mm/day with an interval of 2 mm/day. Models with heat flux adjustment are denoted by (adj). (b) shows the names used in this paper for the different geographical regions.

Figure 3. Annual mean SST averaged between (a) 5N-15N, (b) 5N-5S, and (c) 5S-15S.

Figure 4. Same as Figure 3 but for precipitation.

Figure 5. Meridional profiles of zonal-mean annual mean precipitation.

Figure 6. Interhemispheric difference (5N-15N average minus 5S-15S average) for annual mean (a) SST, and (b) precipitation.

Figure 7. Same as Figure 3 but for τx.

Figure 8. Same as Figure 3 but for LHF.

Figure 9. Same as Figure 3 but for total cloud amount.

Figure 10. Same as Figure 3 but for surface downward shortwave flux (SWF).

Figure 11. Same as Figure 2 but for the AMIP run of 12 models.

Figure 12. Same as Figure 4 but for the AMIP run of 12 models.

Figure 13. Same as Figure 5 but for the AMIP run of 12 models.

Figure 14. Same as Figure 6b but for the AMIP run of 12 models.

Figure 15. Same as Figure 3 but for 5N-5S averaged (a) τx, (b) LHF, and (c) SWF for the AMIP run of 12 models.

Figure 16. Linear regression of 5N-5S averaged monthly data for (a) τx vs zonal SST gradient, (b) zonal precipitation gradient vs zonal SST gradient, (c) zonal pressure gradient vs zonal precipitation gradient, and (d) τx vs zonal pressure gradient force.

Figure 17. Same as Figure 16 but for (a) u vs zonal pressure gradient force, (b) τx vs u, and (c) τx vs u*|V|.

Figure 18. Same as Figure 16 but for (a) τx vs SST, (b) precipitation vs SST, (c) τx vs precipitation, and (d) u vs precipitation.

Figure 19. Same as Figure 16 but for (a) LHF vs SST, (b) | τ | vs SST, (c) sea-air specific humidity difference vs SST, and (d) surface air specific humidity vs SST.

Figure 20. Same as Figure 16 but for (a) SWF vs SST, (b) total cloud amount vs SST, (c) total cloud amount vs SST, and (d) SWF vs total cloud amount.

Figure 21. Same as Figure 16 but for (a) interhemispheric LHF difference (5N-15N average minus 5S-15S average), (b) 5N-15N averaged LHF, and (c) 5S-15S averaged LHF vs interhemispheric SST difference (5N-15N average minus 5S-15S average).

Figure 22. Same as Figure 16 but for 5S-15S averaged (a) SWF vs SST, and (b) total cloud amount vs SST.

Figure 23. Schematic depiction of the tropical mean climate biases in many IPCC AR4 CGCMs. Dark shading denotes excessive precipitation, while light shading denotes insufficient precipitation. Arrow denotes surface zonal wind stress bias. The biases in total cloud amount (CLD), surface downward shortwave flux (SWF), surface latent heat flux (LHF), and SST are denoted by "+" for positive bias, and "-" for negative bias.

Table 1 List of models that participate in this study[1]

Modeling Groups	IPCC ID (Label in Figures)	Grid type/ Resolution/ Model top	Deep convection scheme / Modification	Downdrafts[2] SC/UC/Meso	Closure/ Trigger	Flux correction
National Center for Atmospheric Research	CCSM3 (CCSM3)	Spectral T85*L26 2.2mb	Zhang and McFarlane (1995)	Y/N/N	CAPE	N
National Center for Atmospheric Research	PCM (PCM)	Spectral T42*L26 2.2mb	Zhang and McFarlane (1995)	Y/N/N	CAPE	N
Canadian Centre for Climate Modeling & Analysis	CGCM3.1-T47 (CGCM-T47)	Spectral T47*L32 1mb	Zhang & McFarlane (1995)	Y/N/N	CAPE	Heat, water
Canadian Centre for Climate Modeling & Analysis	CGCM3.1-T63 (CGCM-T63)	Spectral T63*L32 1mb	Zhang & McFarlane (1995)	Y/N/N	CAPE	Heat, water
LASG/Institute of Atmospheric Physics	FGOALS-g1.0 (IAP)	Gridpoint 64*32*L32 2mb	Zhang & McFarlane (1995)	Y/N/N	CAPE	N
NASA/ Goddard Institute for Space Studies	GISS-AOM (GISS-AOM)	Gridpoint 90*60*L12	Russell et al. (1995)	N/N/N	CAPE	N
NASA/ Goddard Institute for Space Studies	GISS-ER (GISS-ER)	Gridpoint 72*46*L20 0.1mb	Del Genio and Yao (1993)	Y/N/N	Cloud base buoyancy	N
NASA/ Goddard Institute for Space Studies	GISS-EH (GISS-EH)	Gridpoint 72*46*L20 0.1mb	Del Genio and Yao (1993)	Y/N/N	Cloud base buoyancy	N
Hadley Centre for Climate Prediction and Research / Met Office	UKMO-HadCM3 (HadCM3)	Spectral T63*L18 4mb	Gregory and Rowntree (1990)	Y/N/N	Cloud base buoyancy	N
Hadley Centre for Climate Prediction and Research / Met Office	UKMO-HadGEM1 (HadGEM1)	Spectral T63*L18 4mb	Gregory and Rowntree (1990)	Y/N/N	Cloud base buoyancy	N
CSIRO Atmospheric Research	CSIRO Mk3.0 (CSIRO)	Spectral T63*L18 4mb	Gregory and Rowntree (1990)	Y/N/N	Cloud base buoyancy	N
Meteorological Research Institute	MRI-CGCM2.3.2 (MRI)	Spectral T42*L30 0.4mb	Pan and Randall (1998)	Y/N/N	CAPE	Heat, water
Center for Climate System Research (The University of Tokyo), National Institute for Environmental Studies, and Frontier Research Center for Global Change	MIROC3.2–hires (MIROC-hires)	Spectral T106*L56	Pan and Randall (1998) / Emori et al. (2001)	Y/N/N	CAPE/ Relative humidity	N
Same as above	MIROC3.2-medres (MIROC-medres)	Spectral T42*L20 30 km	Pan and Randall (1998) / Emori et al. (2001)	Y/N/N	CAPE/ Relative humidity	N

NOAA / Geophysical Fluid Dynamics Laboratory	GFDL-CM2.0 (GFDL2.0)	Gridpoint 144*90*L24 3mb	Moorthi and Suarez (1992) / Tokioka et al. (1988)	N/N/N	CAPE/ Threshold	N
NOAA/ Geophysical Fluid Dynamics Laboratory	GFDL-CM2.1 (GFDL2.1)	Gridpoint 144*90*L24 3mb	Moorthi and Suarez (1992) / Tokioka et al. (1988)	N/N/N	CAPE/ Threshold	N
Max Planck Institute for Meteorology	ECHAM5/ MPI-OM (MPI)	Spectral T63*L31 10mb	Tiedtke (1989) / Nordeng (1994)	Y/N/N	CAPE/ Moisture convergence	N
Meteorological Institute of the University of Bonn, Meteorological Research Institute of KMA, and Model and Data Group	ECHO-G (ECHO-G)	Spectral T30*L19 10mb	Tiedtke (1989) / Nordeng (1994)	Y/N/N	CAPE/ Moisture convergence	Heat, water
Mateo-France / Centre National de Recherches Météorologiques	CNRM-CM3 (CNRM)	Spectral T63*L45 0.05mb	Bougeault (1985)	N/N/N	Kuo	N
Bjerknes Centre for Climate Research	BCCR-BCM2.0 (BCCR)	Spectral T63*L31 10mb	Bougeault (1985)	N/N/N	Kuo	N
Institute for Numerical Mathematics	INM-CM3.0 (INM)	Gridpoint 72*45*L21	Betts (1986)	N/N/N	CAPE	Water
Institute Pierre Simon Laplace	IPSL-CM4 (IPSL)	Gridpoint 96*72*L19	Emanuel (1991)	Y/Y/N	CAPE	N

[1]Models with same or similar deep convection schemes are listed together.
[2]For downdrafts, SC means saturated convective downdrafts, UC means unsaturated convective downdrafts, and Meso means mesoscale downdrafts.

Table 2. Observational datasets used in this study

Variable (Acronym)	Dataset	Spatial Coverage/ Resolution (degrees)	Temporal Coverage	Reference
Sea surface temperature (SST)	ERSST	Global ocean 1x1	1979-2004	Smith and Reynolds 2004
	HADISST	Global ocean 1x1	1979-2004	Rayner et al. 2003
Precipitation	GPCP	Global 2.5x2.5	1979-2004	Adler et al. 2003
	TRMM PR/TMI combined	Global 5x5	1998-2005	
Sea level pressure (SLP); surface zonal wind stress (τ_x)	NCEP/NCAR reanalysis	Global 2.5x2.5	1979-1999	Kalnay et al. 1996
	ERA-40 reanalysis	Global 2.5x2.5	1979-1999	Gibson et al. 1997
Surface latent heat flux	NCEP/NCAR reanalysis	Global 2.5x2.5	1979-1999	Kalnay et al. 1996
Total cloud amount	ISCCP D2	Global 2.5x2.5	1984-2000	Rossow et al. 1996
Surface net shortwave flux	ISCCP derived	Global 2.5x2.5	1984-2002	Zhang et al. 2004

Table 3. AGCM biases in ocean-atmosphere feedback parameters

IPCC ID (Label in Figures)	Insufficient equatorial Pacific precipitation in coupled run?	Excessive Bjerknes feedback?	Overly positive SST-LHF feedback?	Insufficient SST-SWF feedback?
CCSM3 (CCSM3)			Y	Excessive
PCM (PCM)	Y		Y	Y
FGOALS-g1.0 (IAP)	Y			
GISS-ER (GISS-ER)		Y	Y	
UKMO-HadGEM1 (HadGEM1)	Y	Y		
MRI-CGCM2.3.2 (MRI)	Heat flux correction	Y	Overly negative	Excessive
MIROC3.2–medres (MIROC-hires)			Overly negative	Y
MIROC3.2-hires (MIROC-medres)				Y
ECHAM5/MPI-OM (MPI)	Y	Y		Excessive
CNRM-CM3 (CNRM)	Y	Y	Y	Excessive
INM-CM3.0 (INM)	Y	Y	Y	Excessive
IPSL-CM4 (IPSL)				Excessive

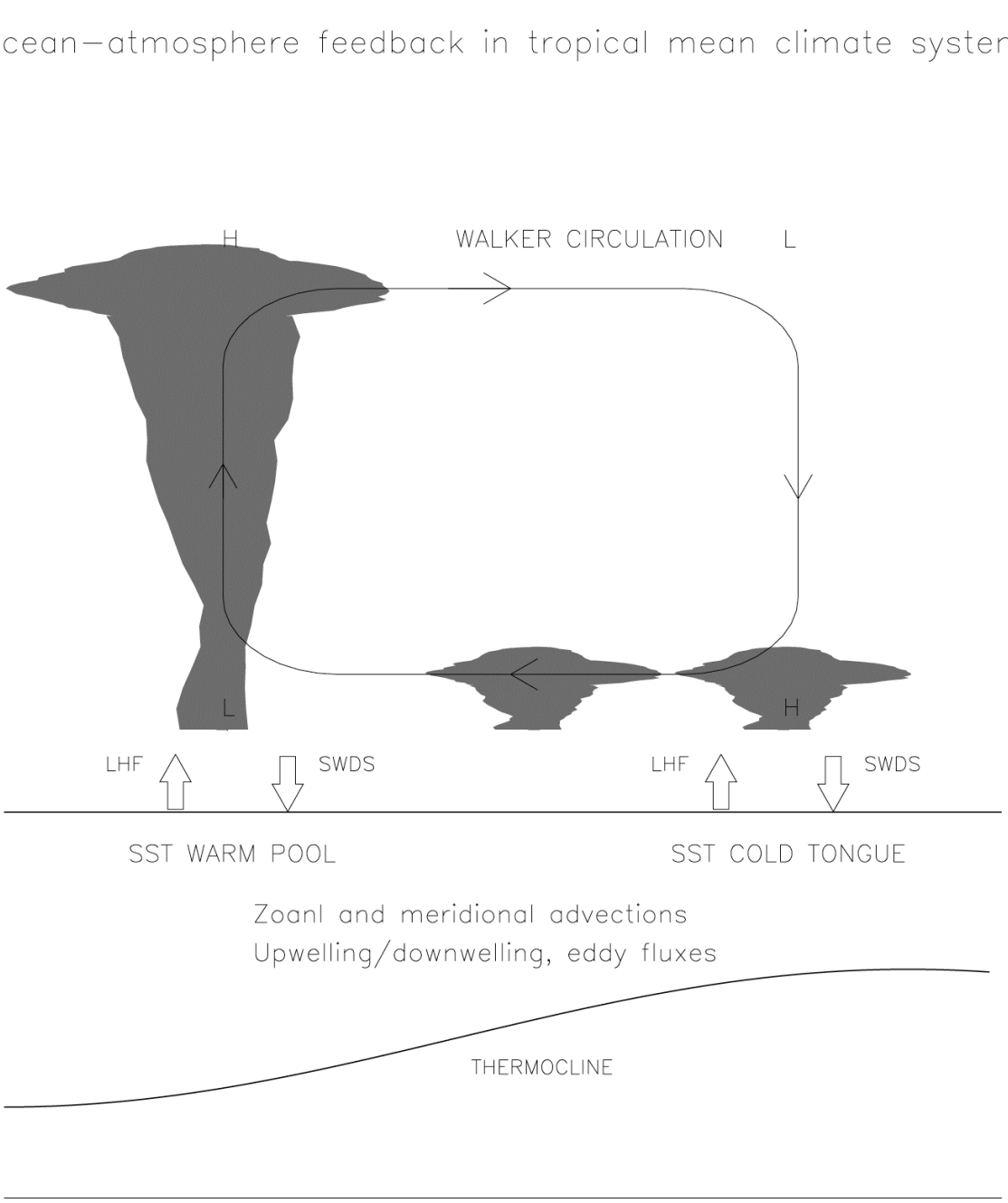

Figure 1. Schematic depiction of the ocean-atmosphere feedback mechanisms in tropical mean climate system.

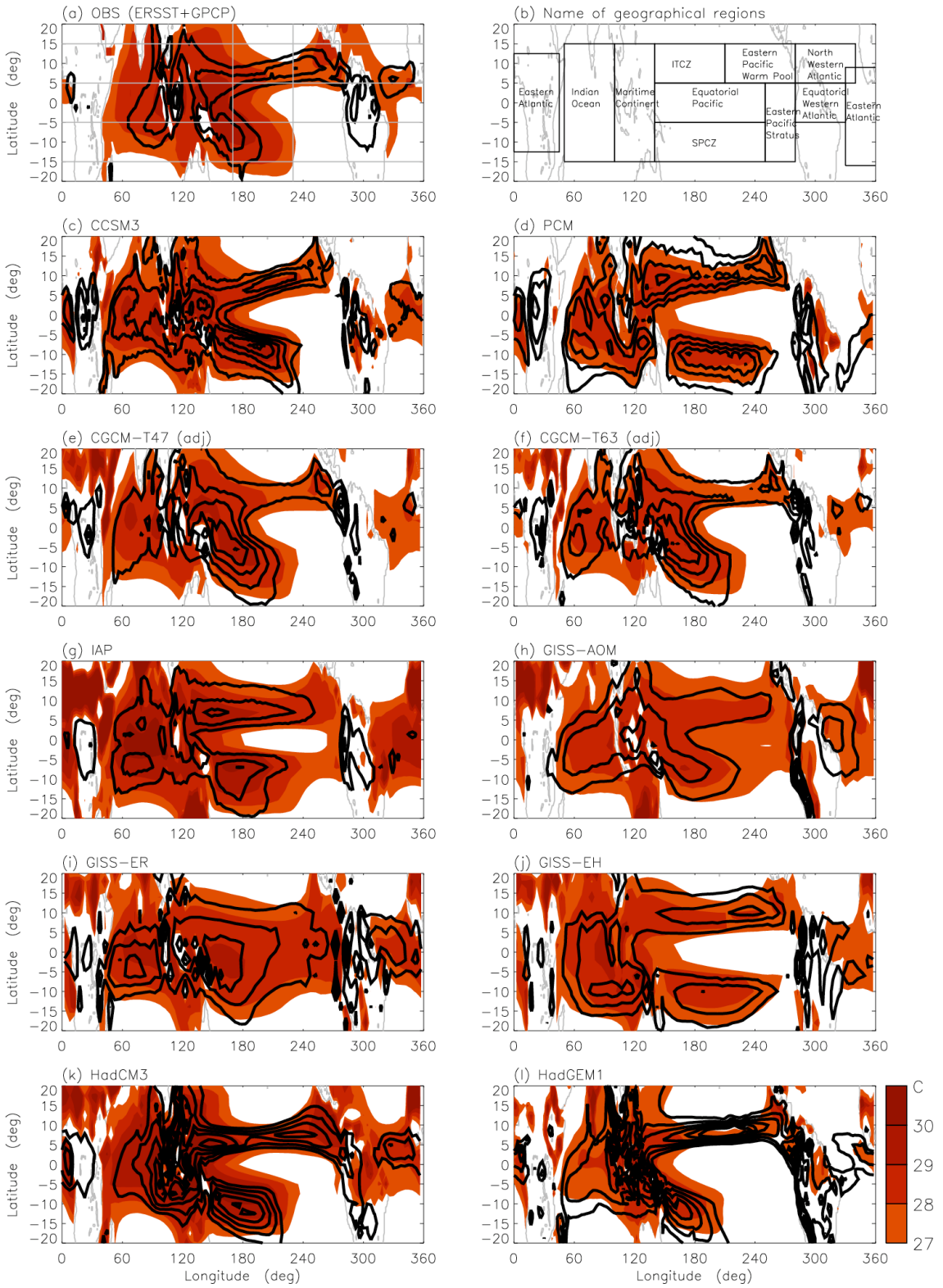

Figure 2. Annual mean SST (shading) and precipitation (contour) for observation and 22 IPCC AR4 CGCMs. Contour starts at 5 mm/day with an interval of 2 mm/day. Models with heat flux adjustment are denoted by (adj). (b) shows the names used in this paper for the different geographical regions.

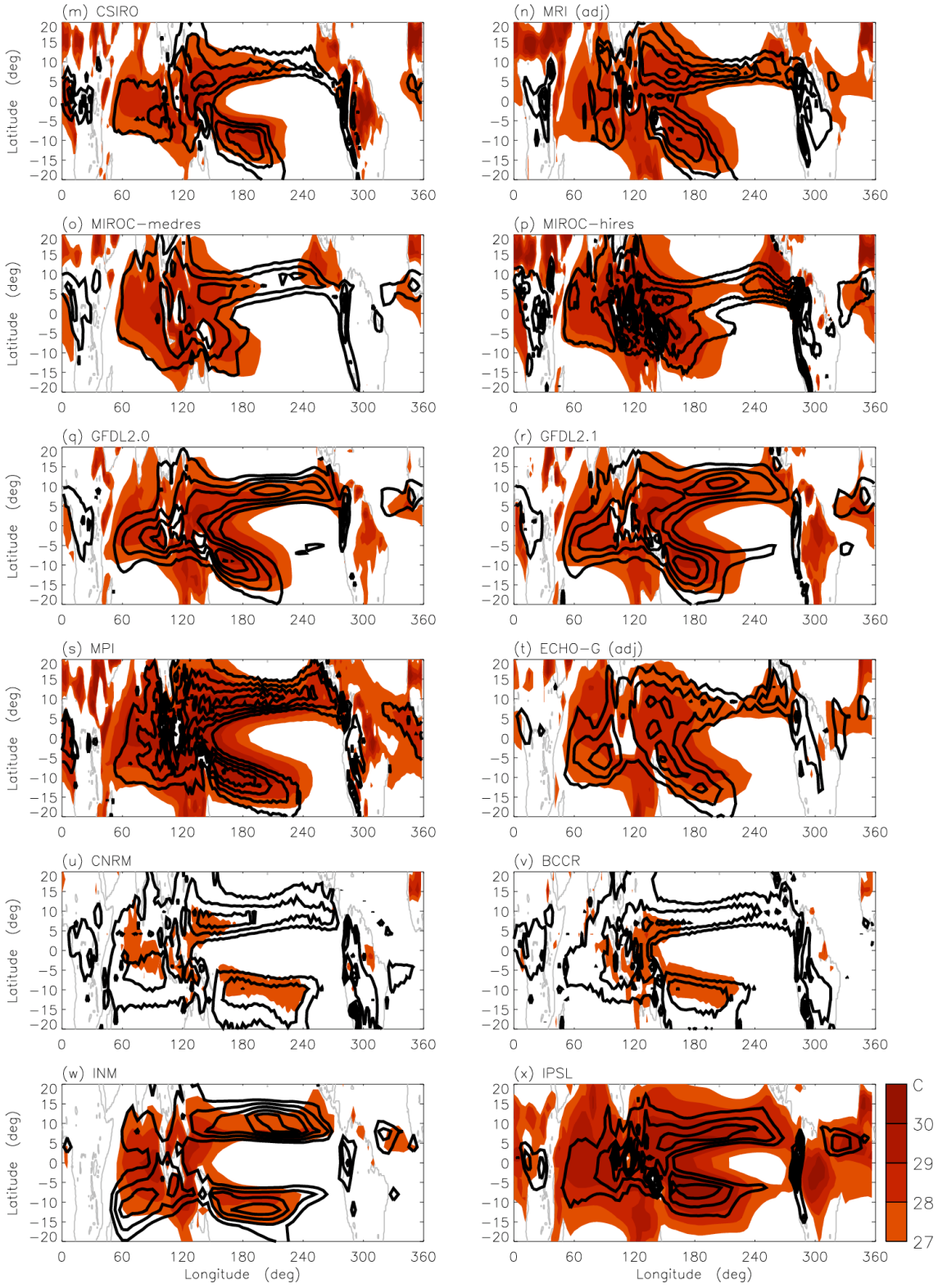

Figure 2. Continued.

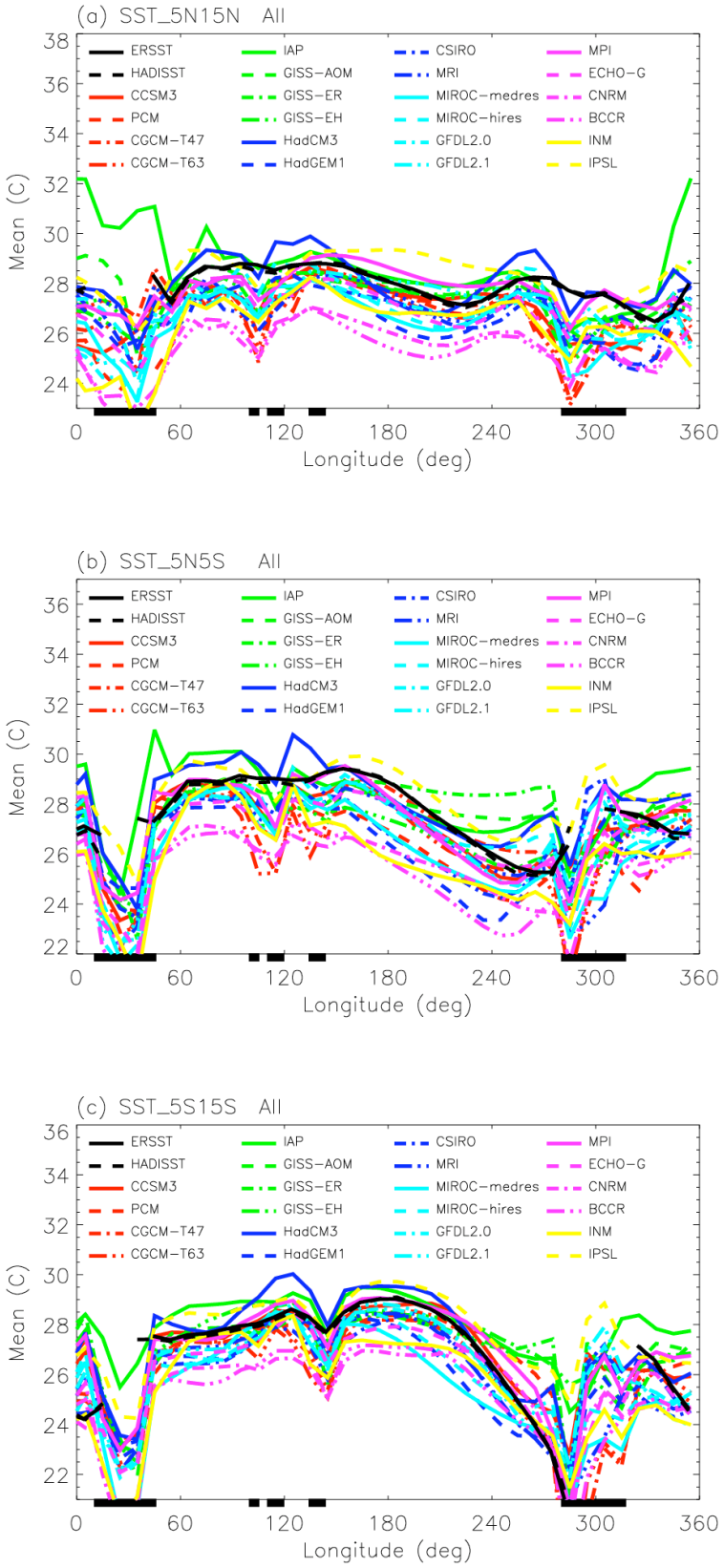

Figure 3. Annual mean SST averaged between (a) 5N-15N, (b) 5N-5S, and (c) 5S-15S.

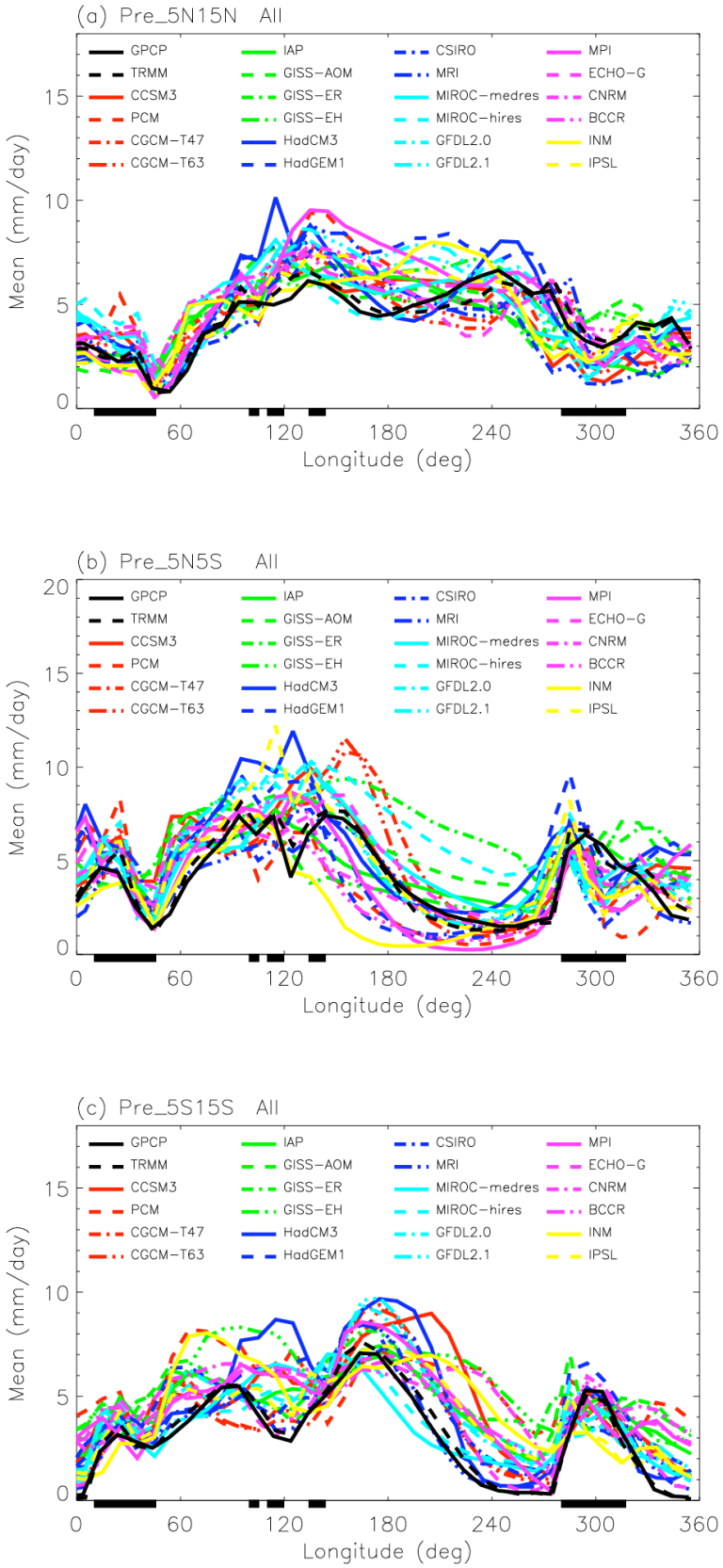

Figure 4. Same as Figure 3 but for precipitation.

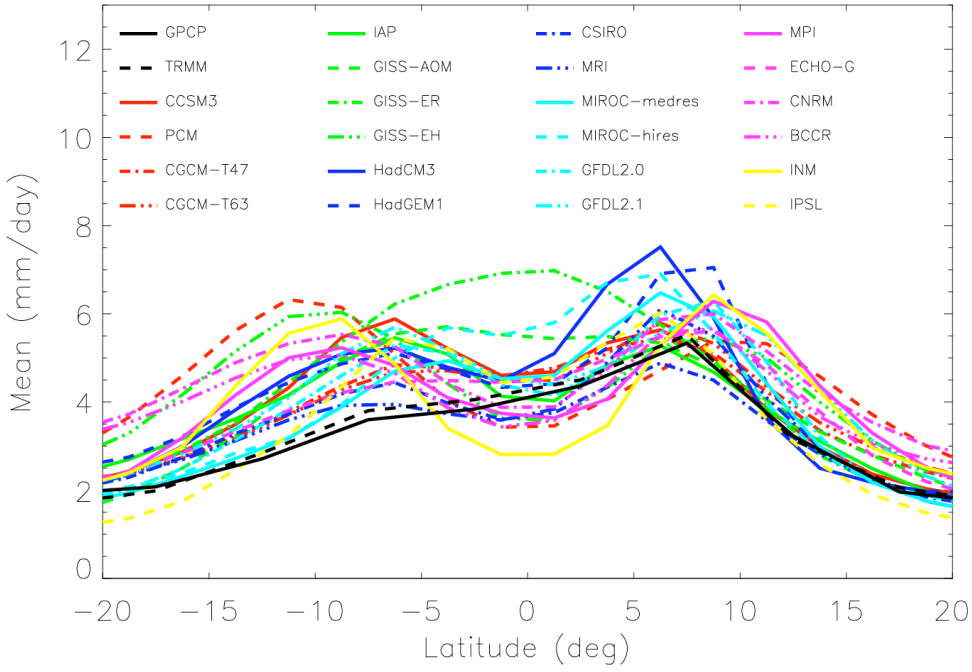

Figure 5. Meridional profiles of zonal-mean annual mean precipitation.

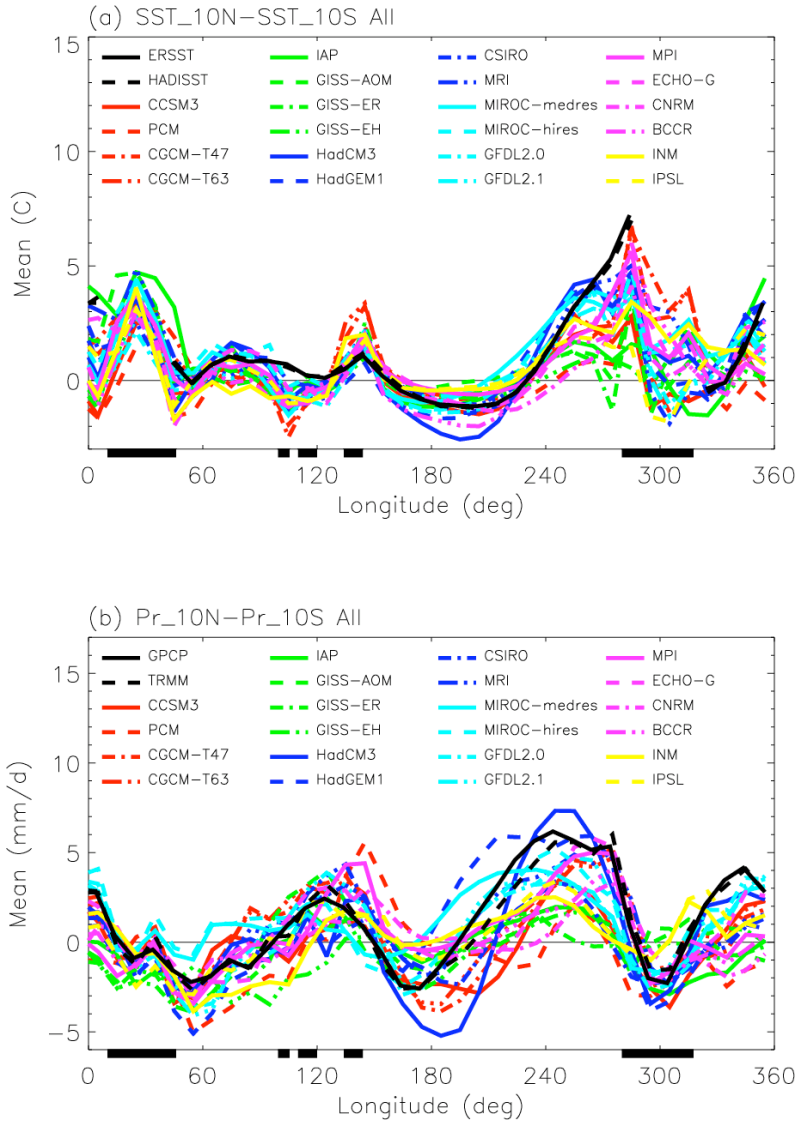

Figure 6. Interhemispheric difference (5N-15N average minus 5S-15S average) for annual mean (a) SST, and (b) precipitation.

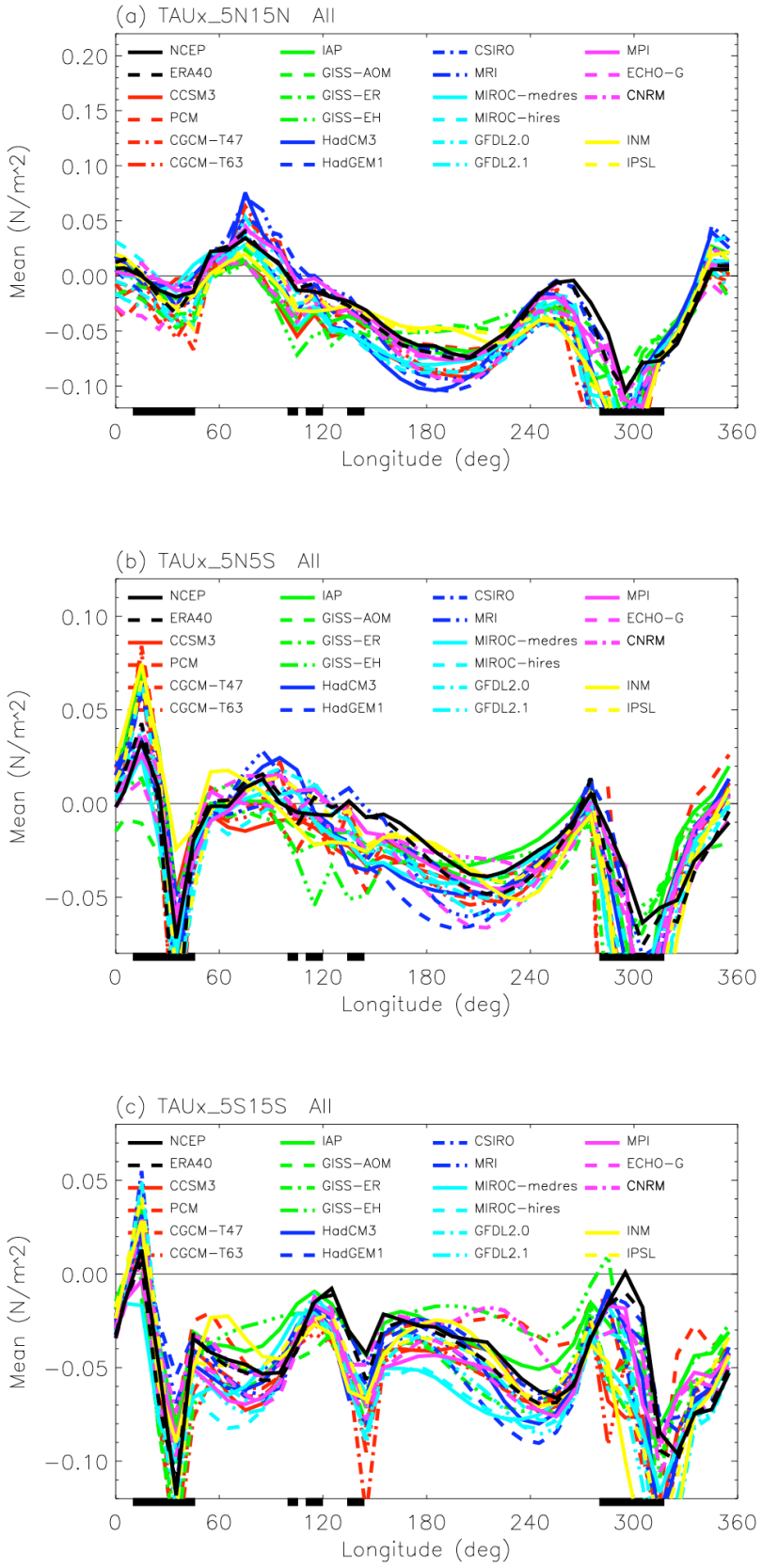

Figure 7. Same as Figure 3 but for τ_x.

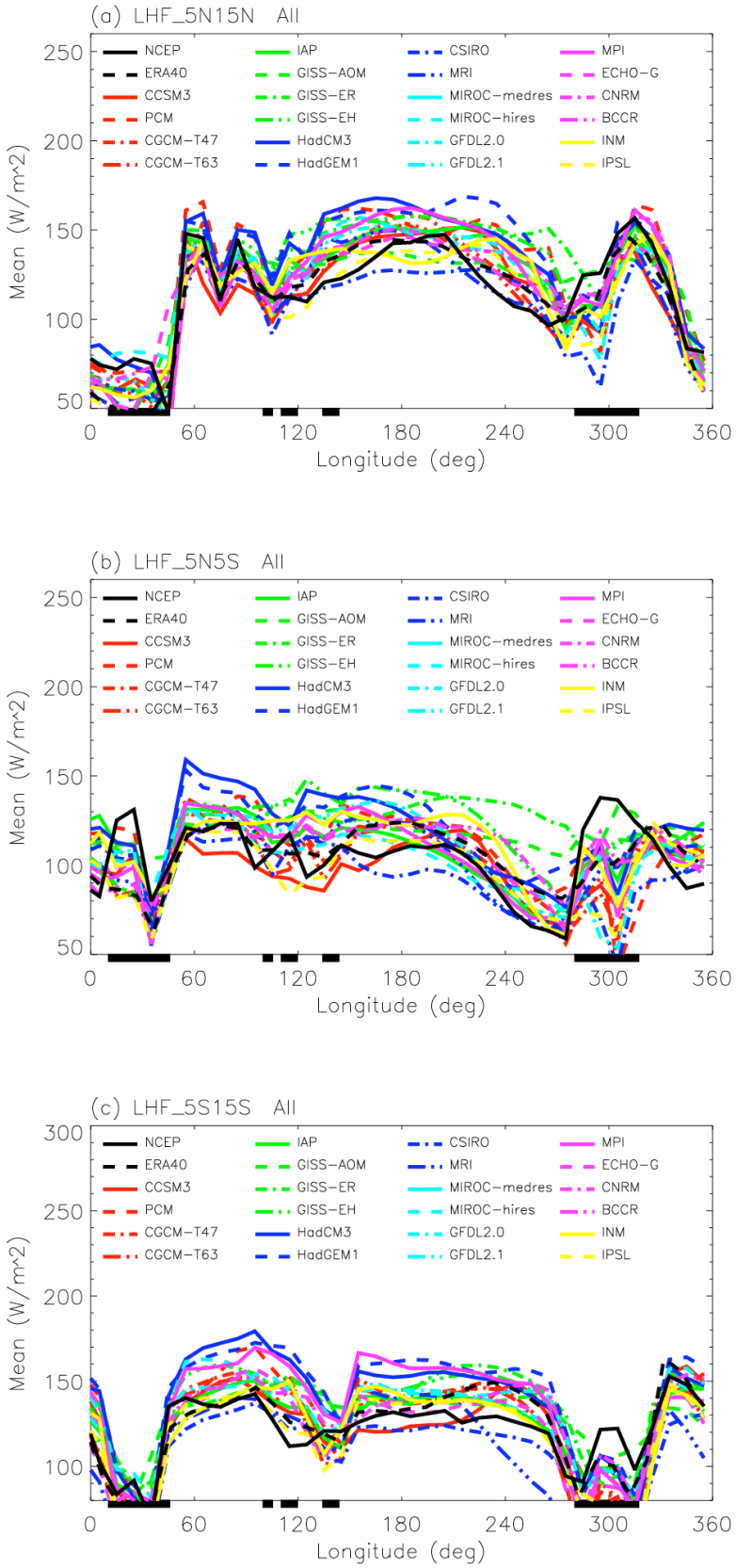

Figure 8. Same as Figure 3 but for LHF.

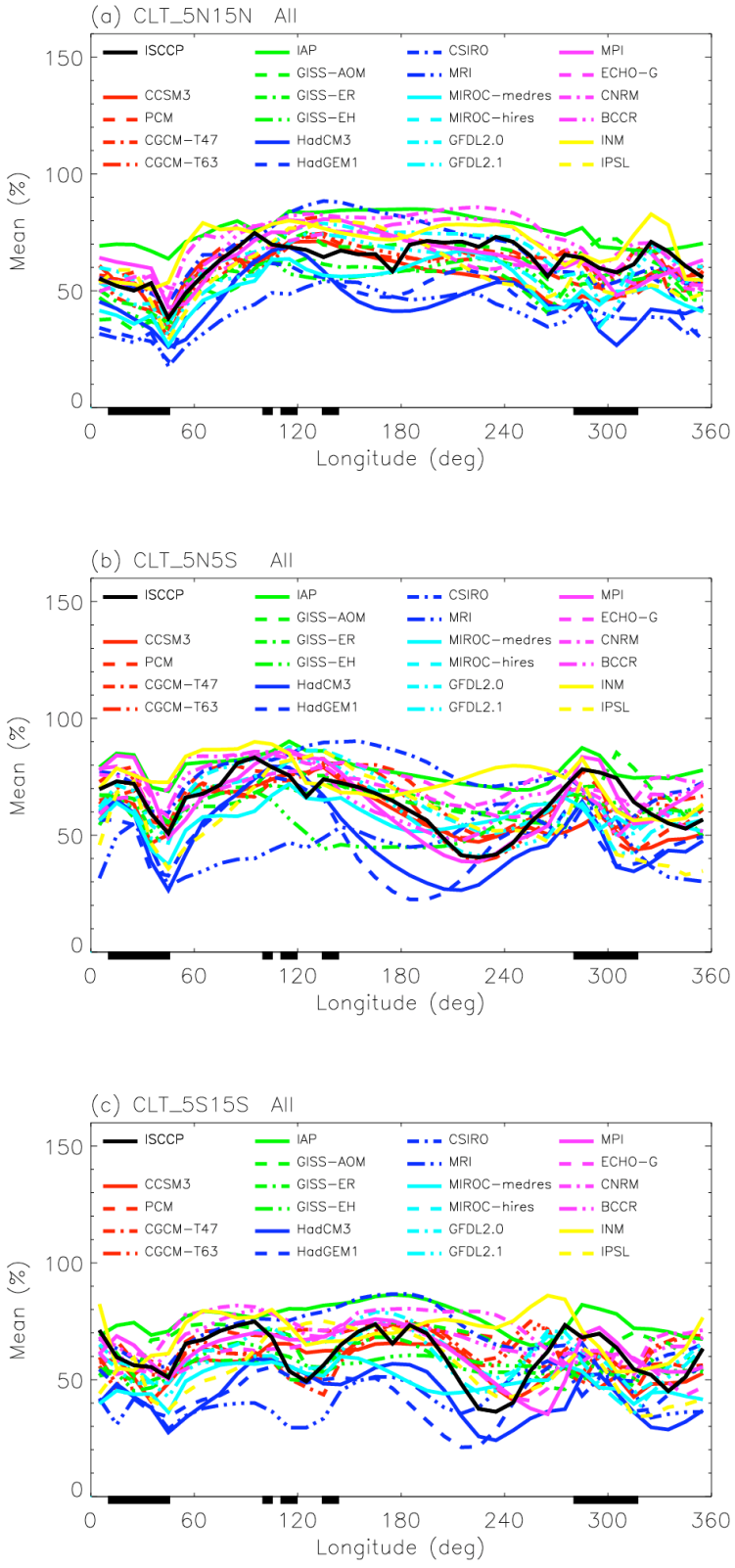

Figure 9. Same as Figure 3 but for total cloud amount.

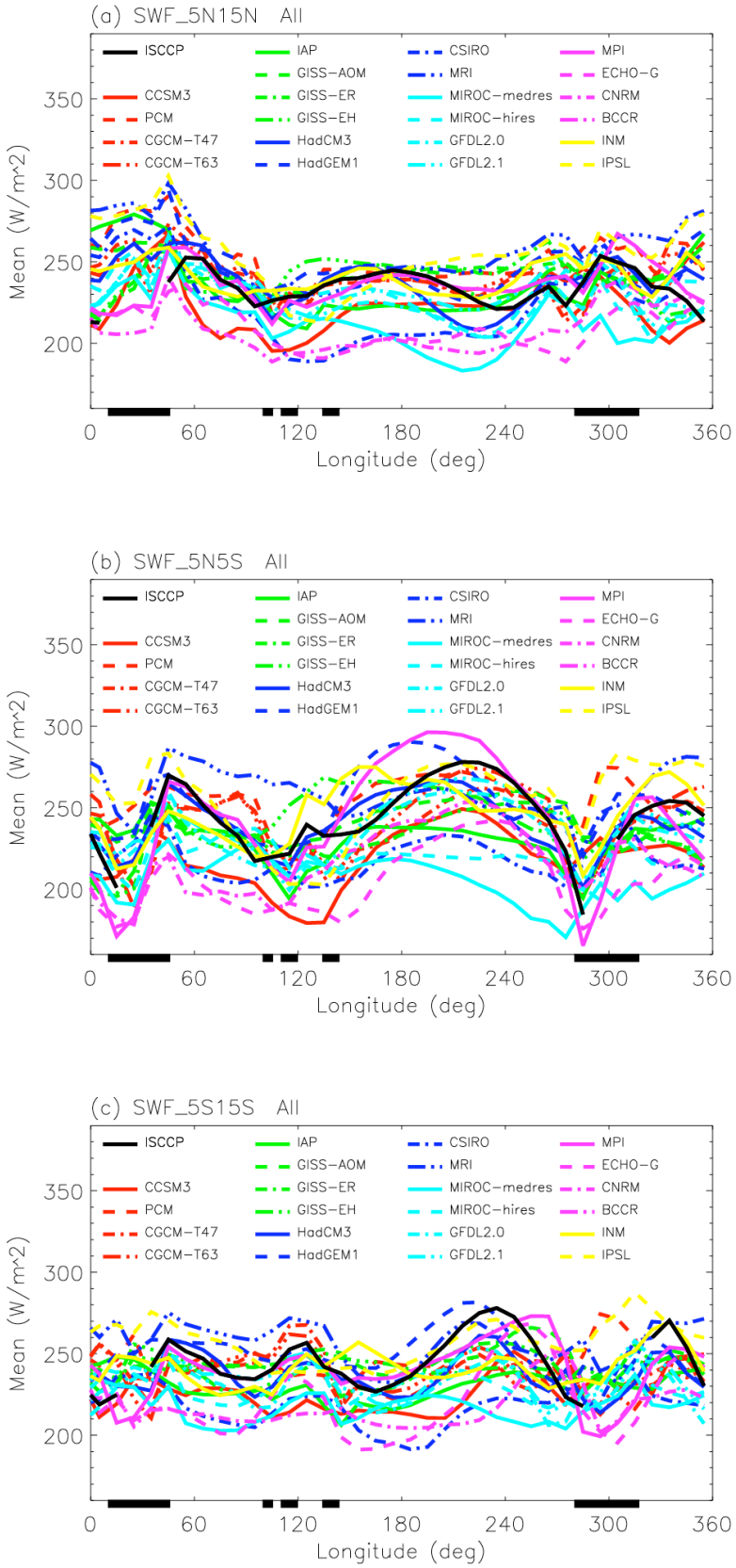

Figure 10. Same as Figure 3 but for surface downward shortwave flux (SWF).

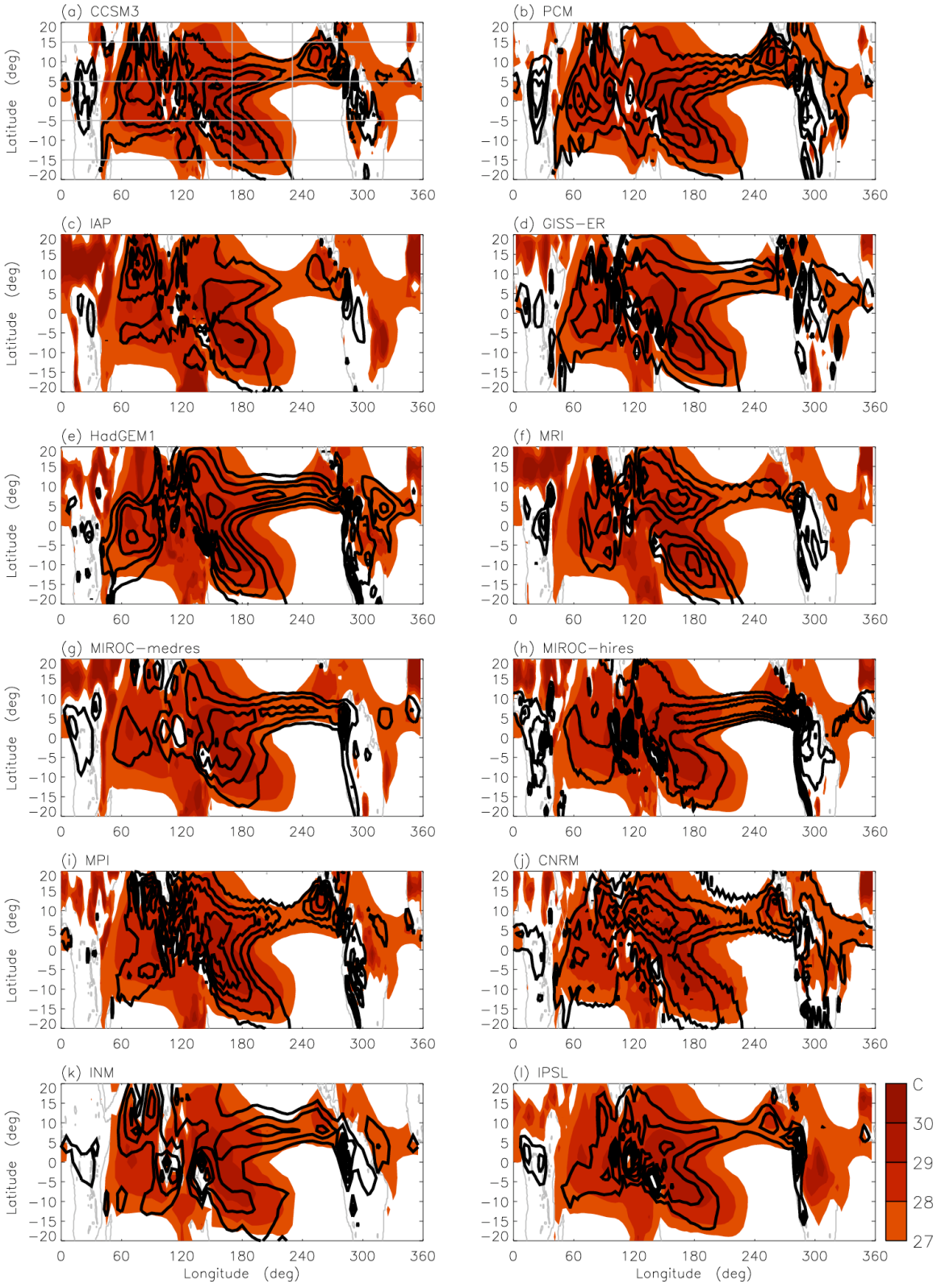

Figure 11. Same as Figure 2 but for the AMIP run of 12 models.

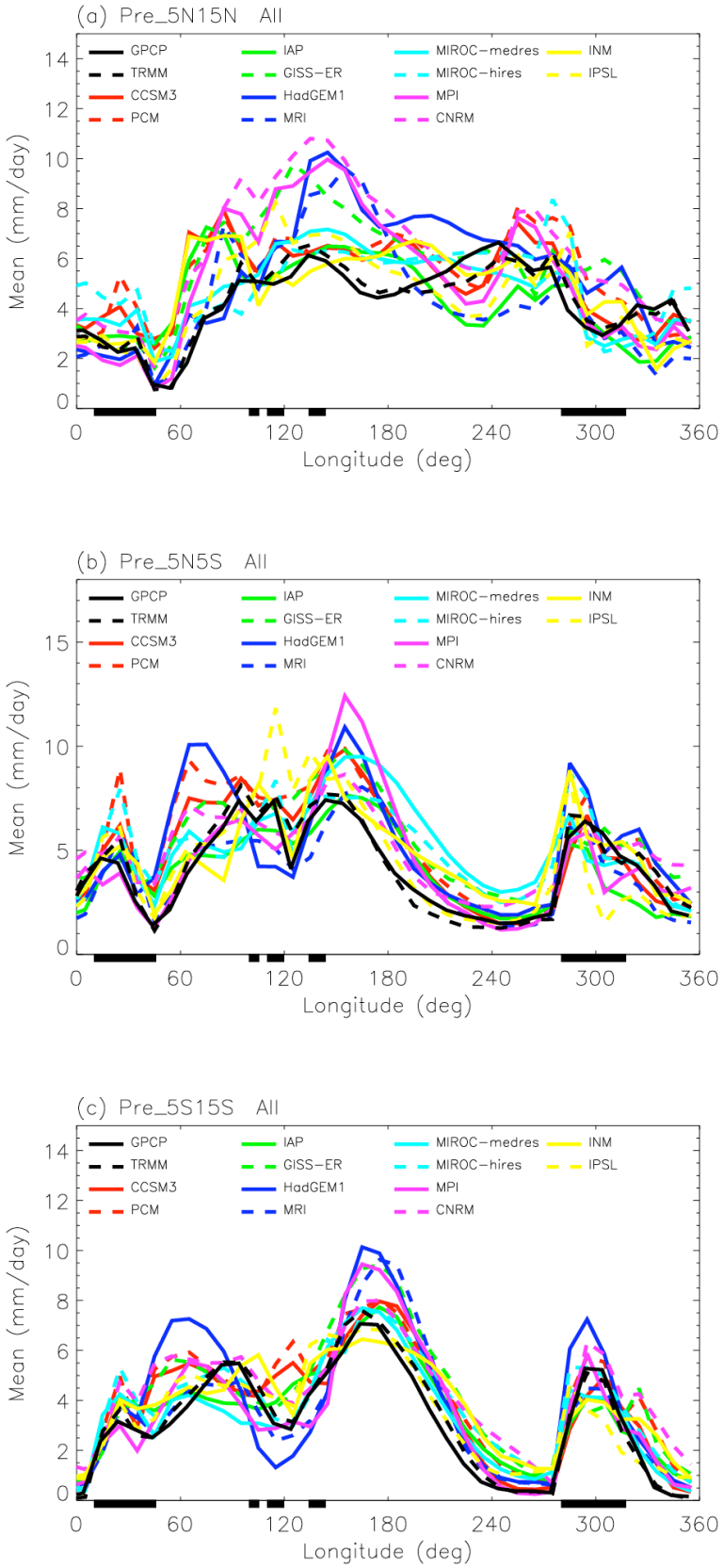

Figure 12. Same as Figure 4 but for the AMIP run of 12 models.

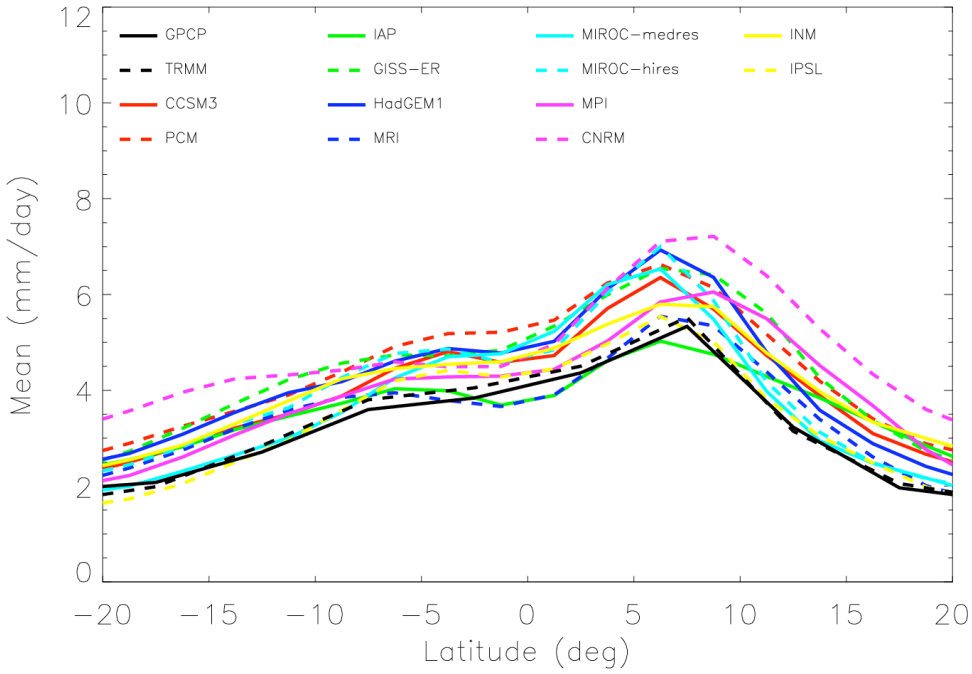

Figure 13. Same as Figure 5 but for the AMIP run of 12 models.

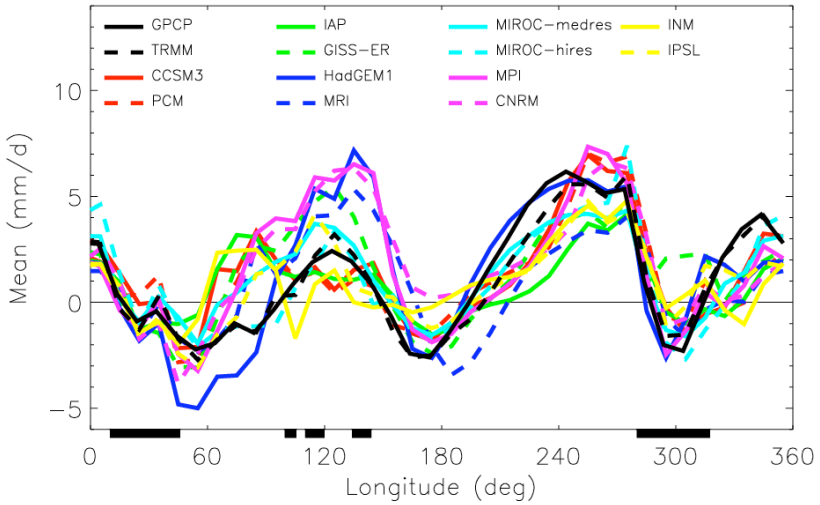

Figure 14. Same as Figure 6b but for the AMIP run of 12 models.

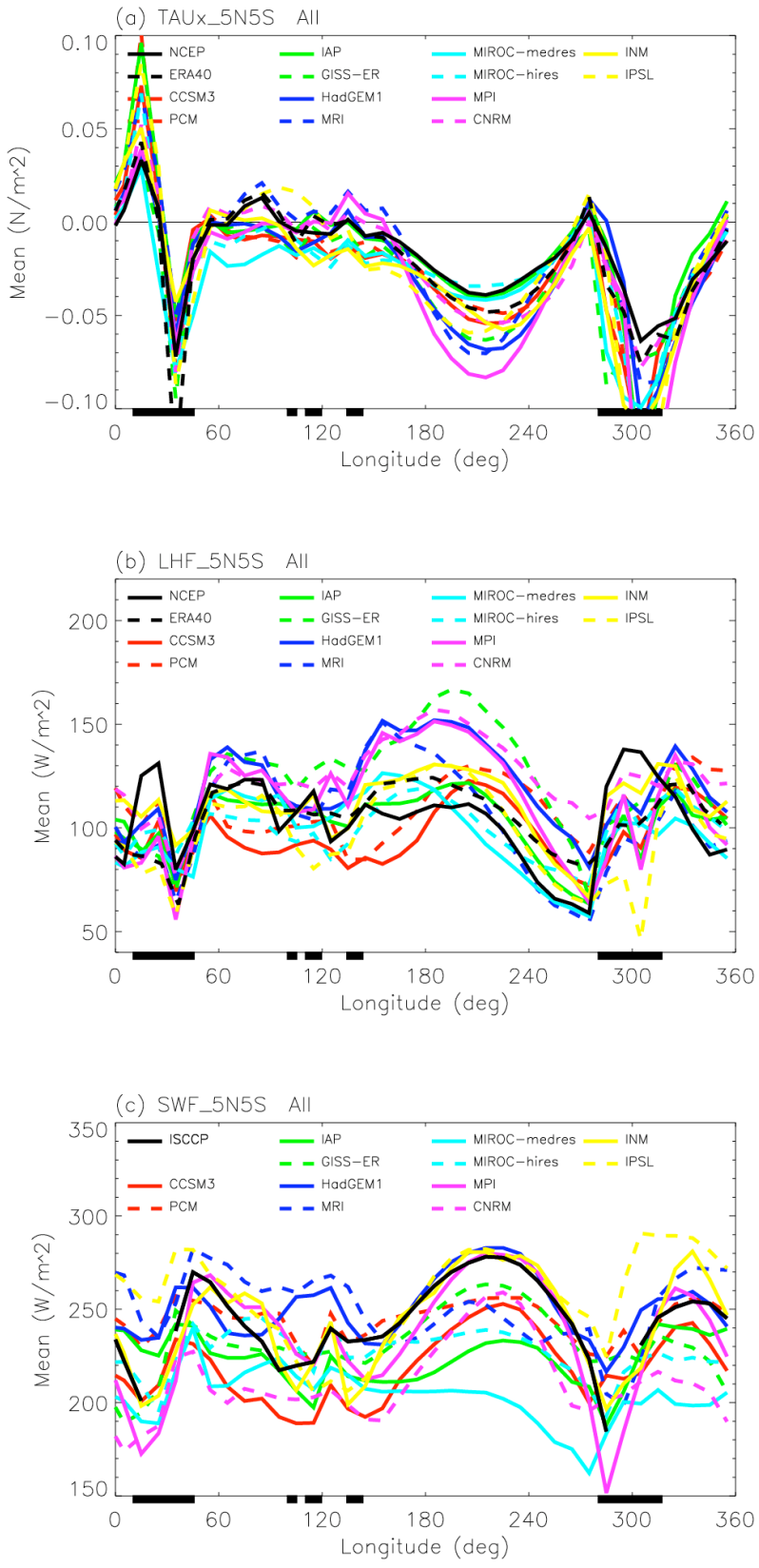

Figure 15. Same as Figure 3 but for 5N-5S averaged (a) τ_x, (b) LHF, and (c) SWF for the AMIP run of 12 models.

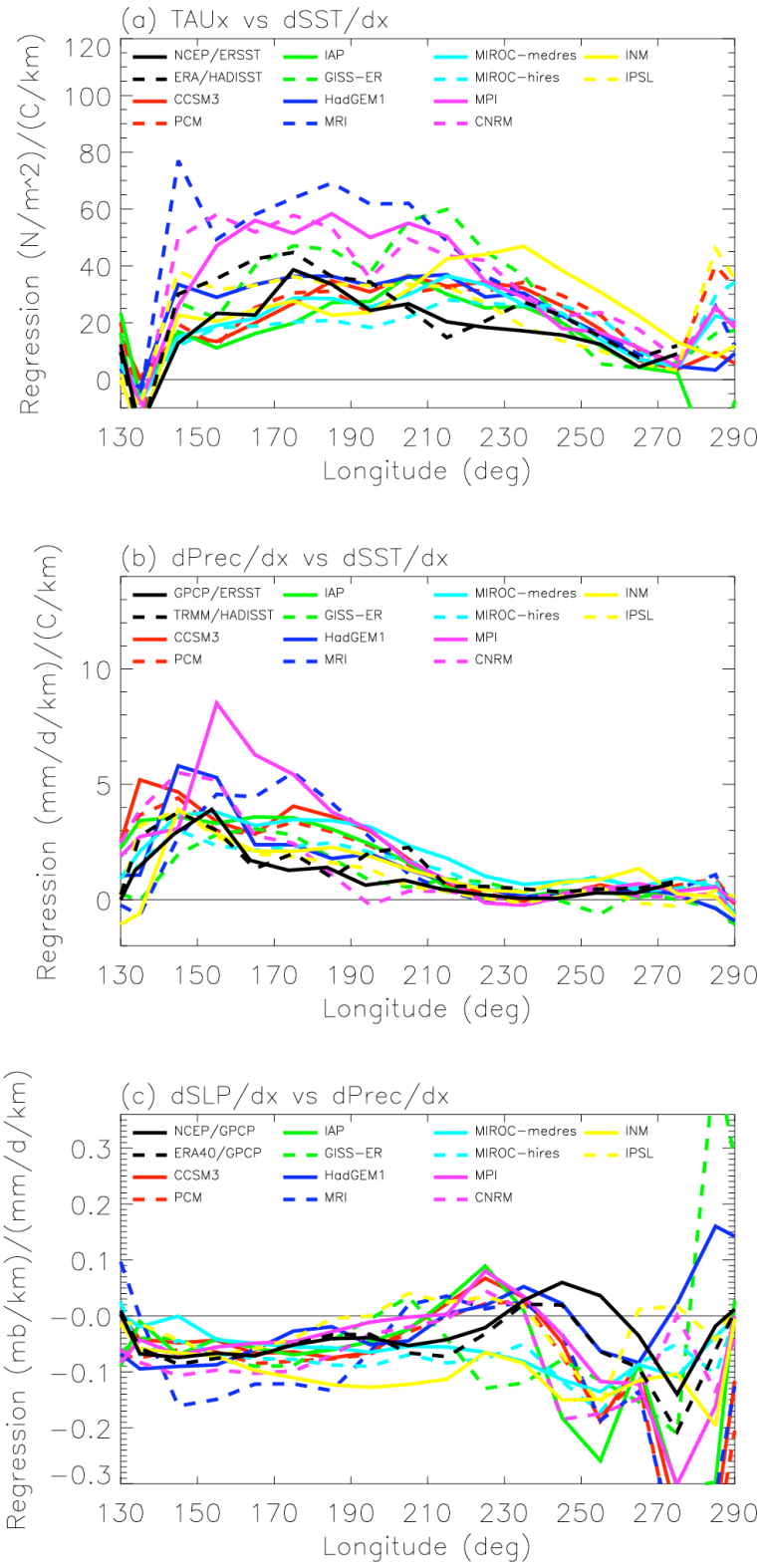

Figure 16. Linear regression of 5N-5S averaged monthly data for (a) τ_x vs zonal SST gradient, (b) zonal precipitation gradient vs zonal SST gradient, (c) zonal pressure gradient vs zonal precipitation gradient, and (d) τ_x vs zonal pressure gradient force.

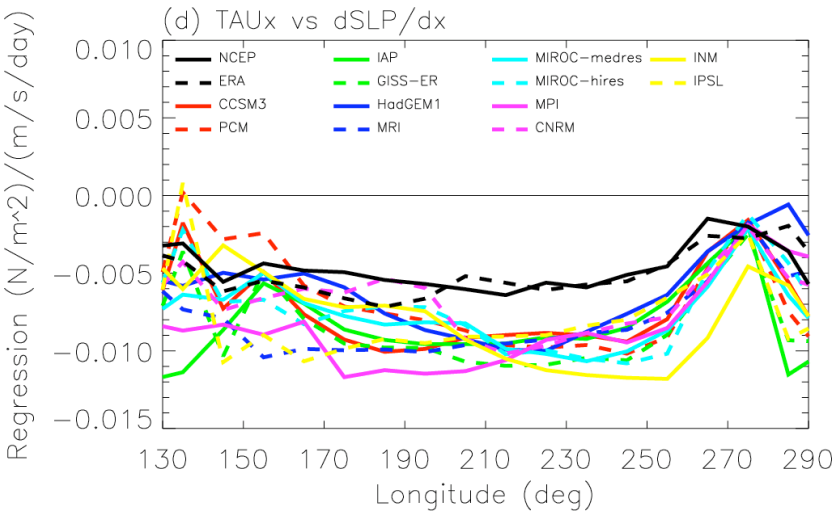

Figure 16. Continued.

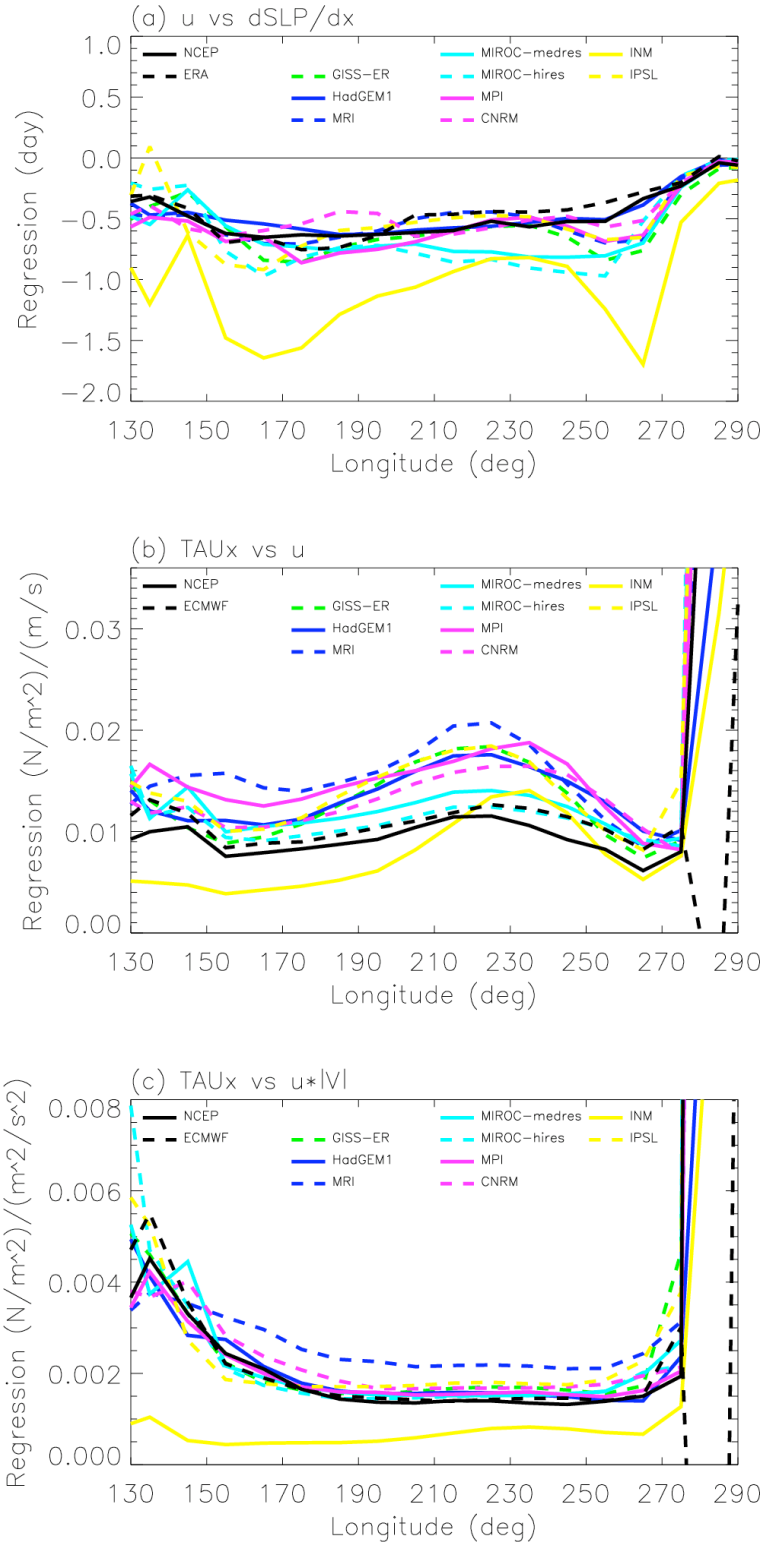

Figure 17. Same as Figure 16 but for (a) u vs zonal pressure gradient force, (b) τ_x vs u, and (c) τ_x vs u*|V|.

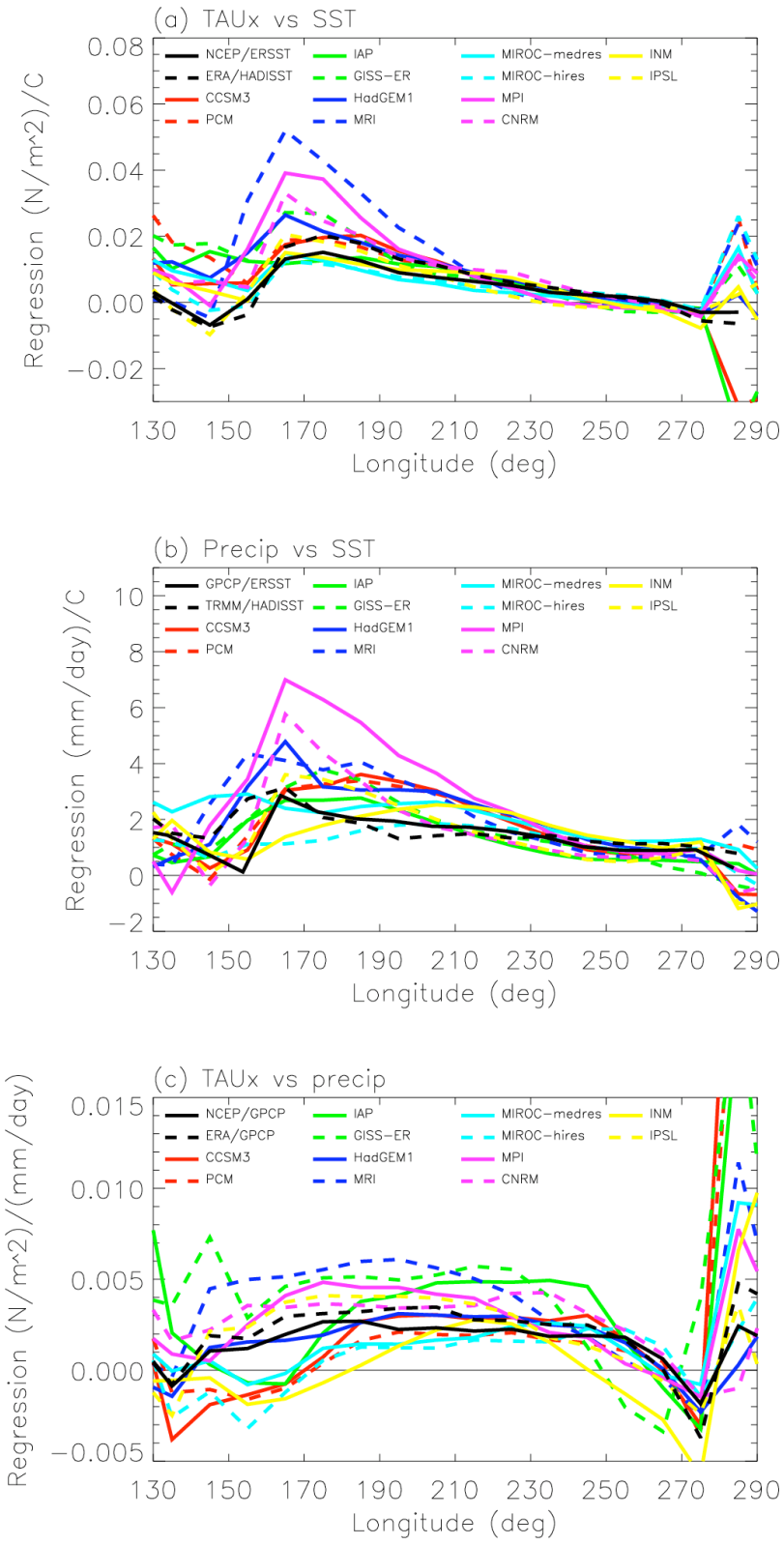

Figure 18. Same as Figure 16 but for (a) τ_x vs SST, (b) precipitation vs SST, (c) τ_x vs precipitation, and (d) u vs precipitation.

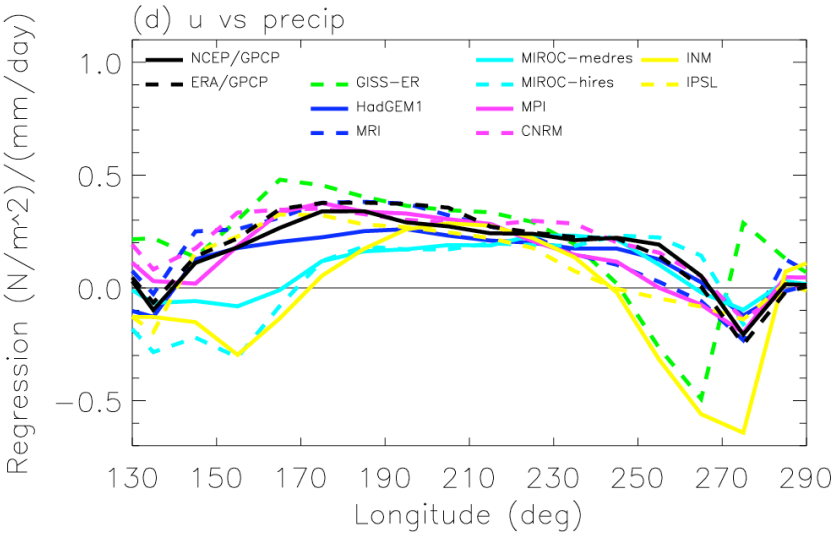

Figure 18. Continued.

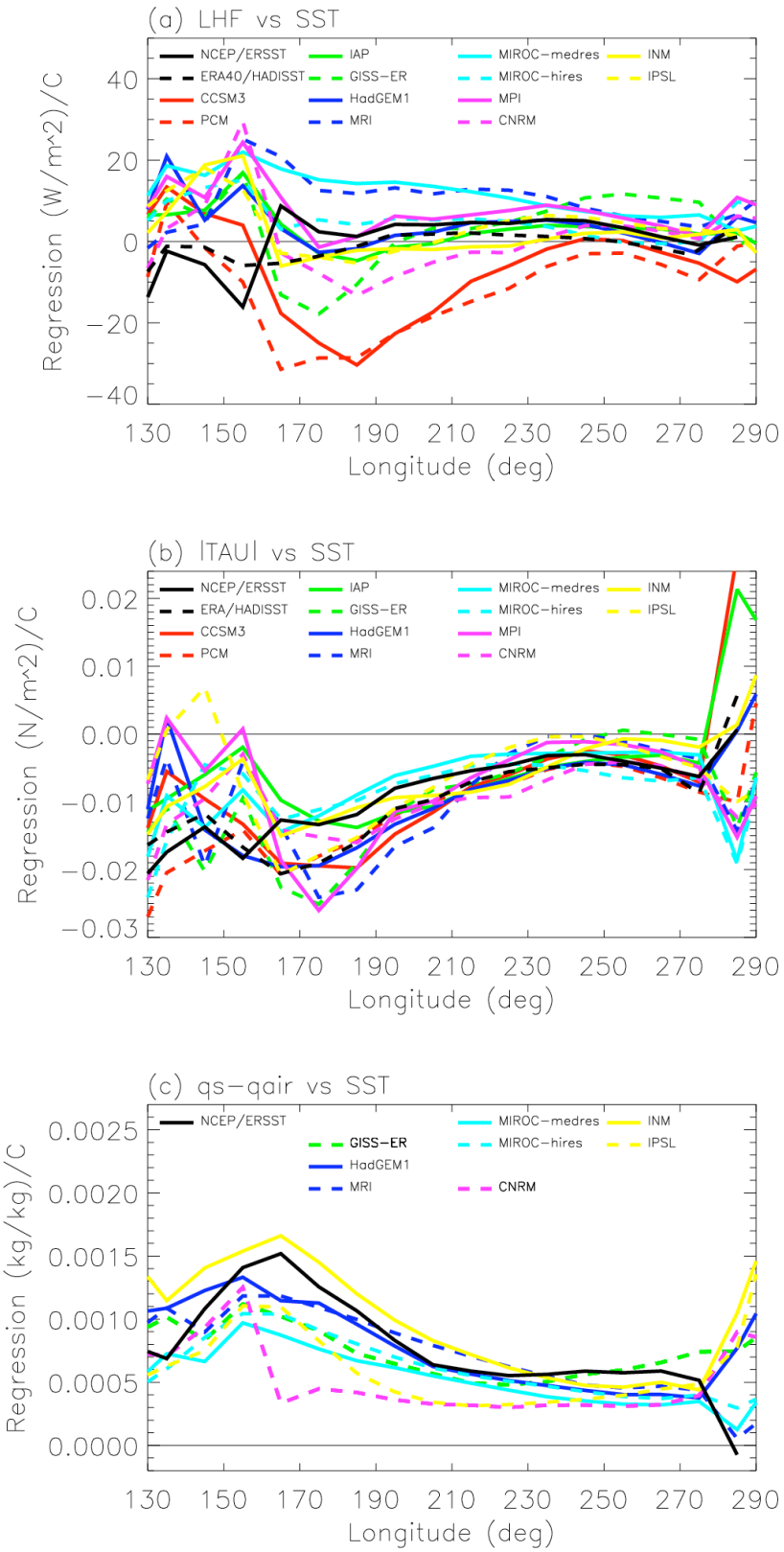

Figure 19. Same as Figure 16 but for (a) LHF vs SST, (b) | τ | vs SST, (c) sea-air specific humidity difference vs SST, and (d) surface air specific humidity vs SST. In (c) and (d), surface air specific humidity data is not available for four models.

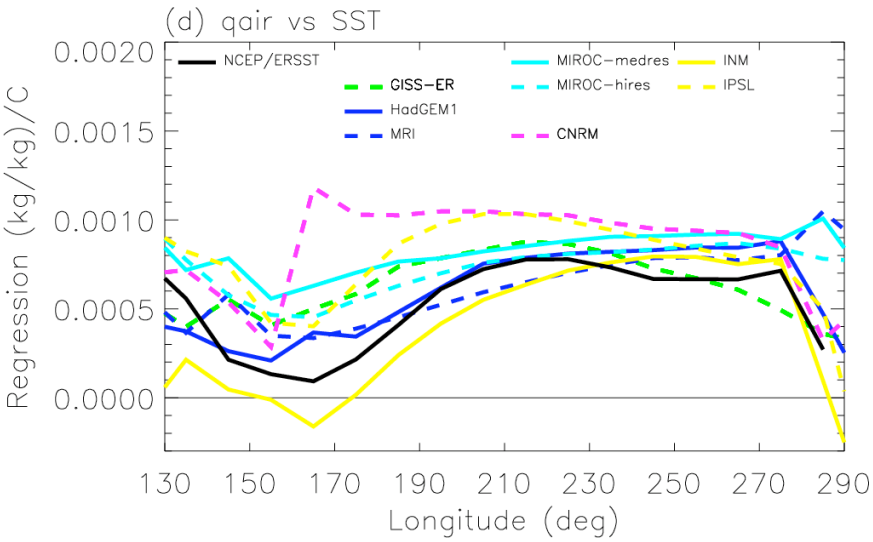

Figure 19. Continued.

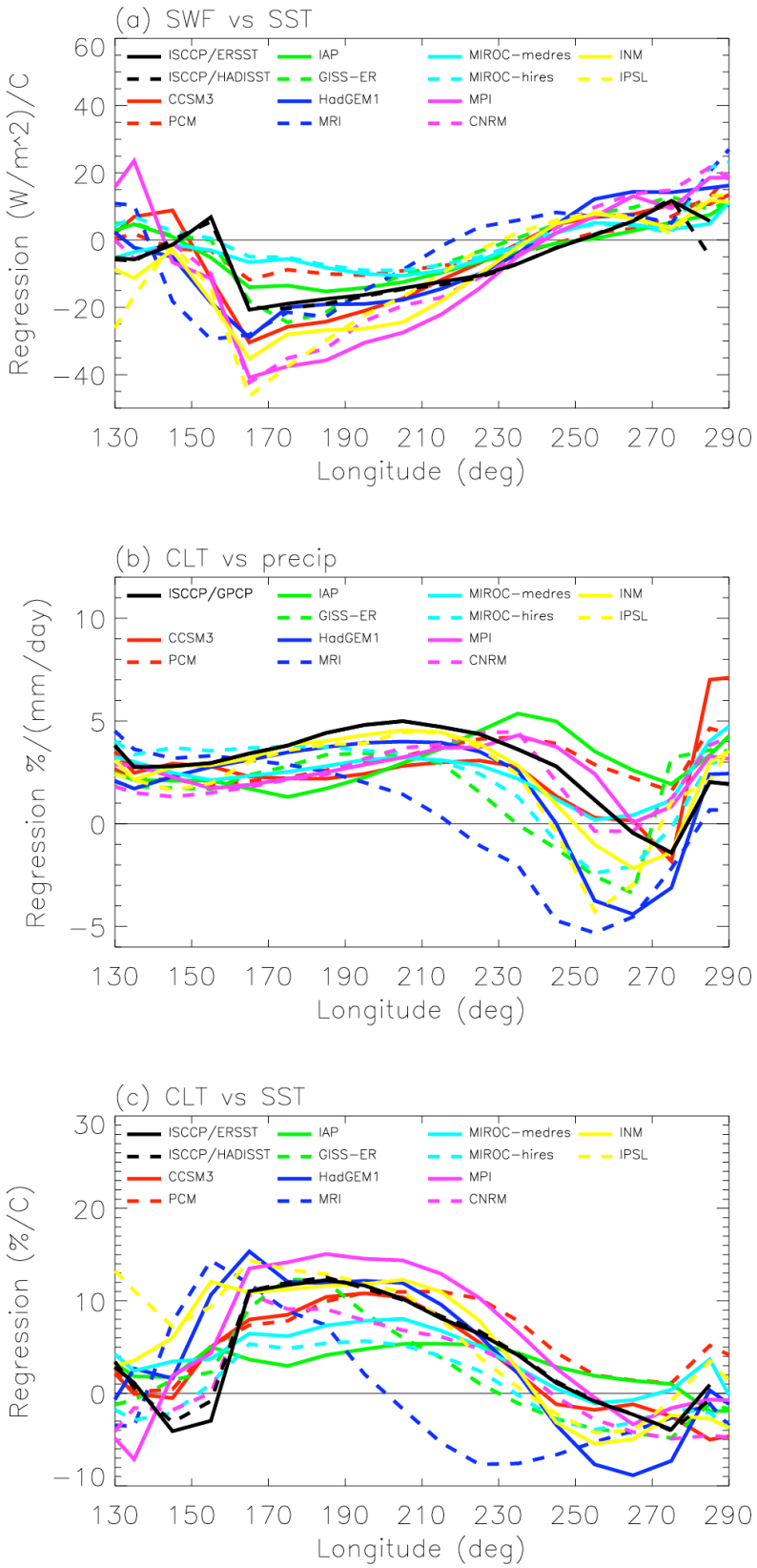

Figure 20. Same as Figure 16 but for (a) SWF vs SST, (b) total cloud amount vs SST, (c) total cloud amount vs SST, and (d) SWF vs total cloud amount.

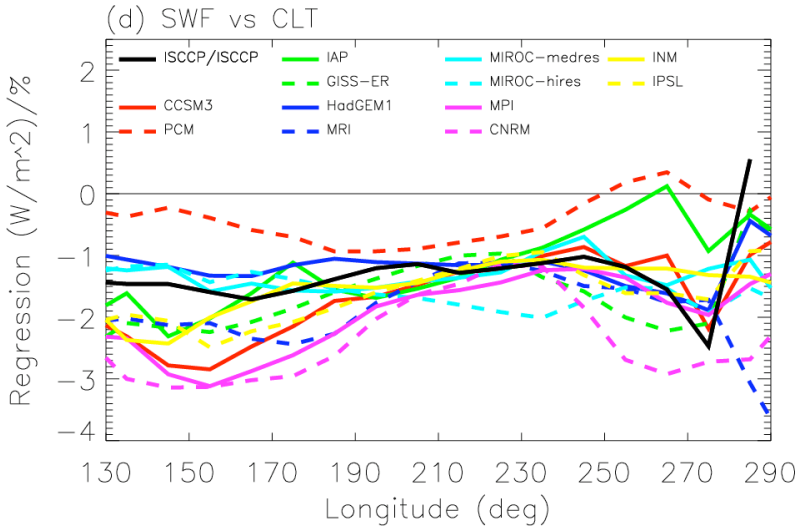

Figure 20. Continued.

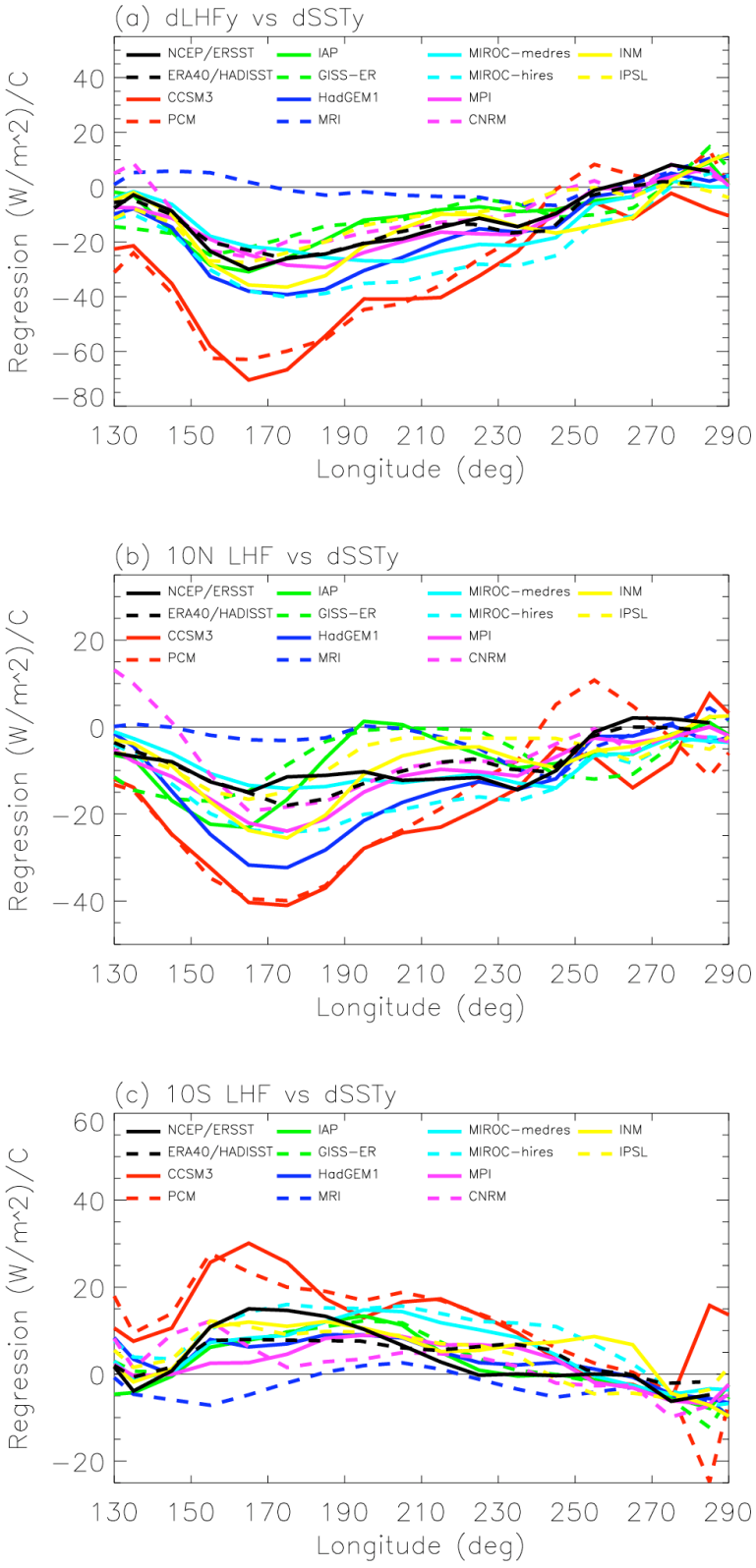

Figure 21. Same as Figure 16 but for (a) interhemispheric LHF difference (5N-15N average minus 5S-15S average), (b) 5N-15N averaged LHF, and (c) 5S-15S averaged LHF vs interhemispheric SST difference (5N-15N average minus 5S-15S average).

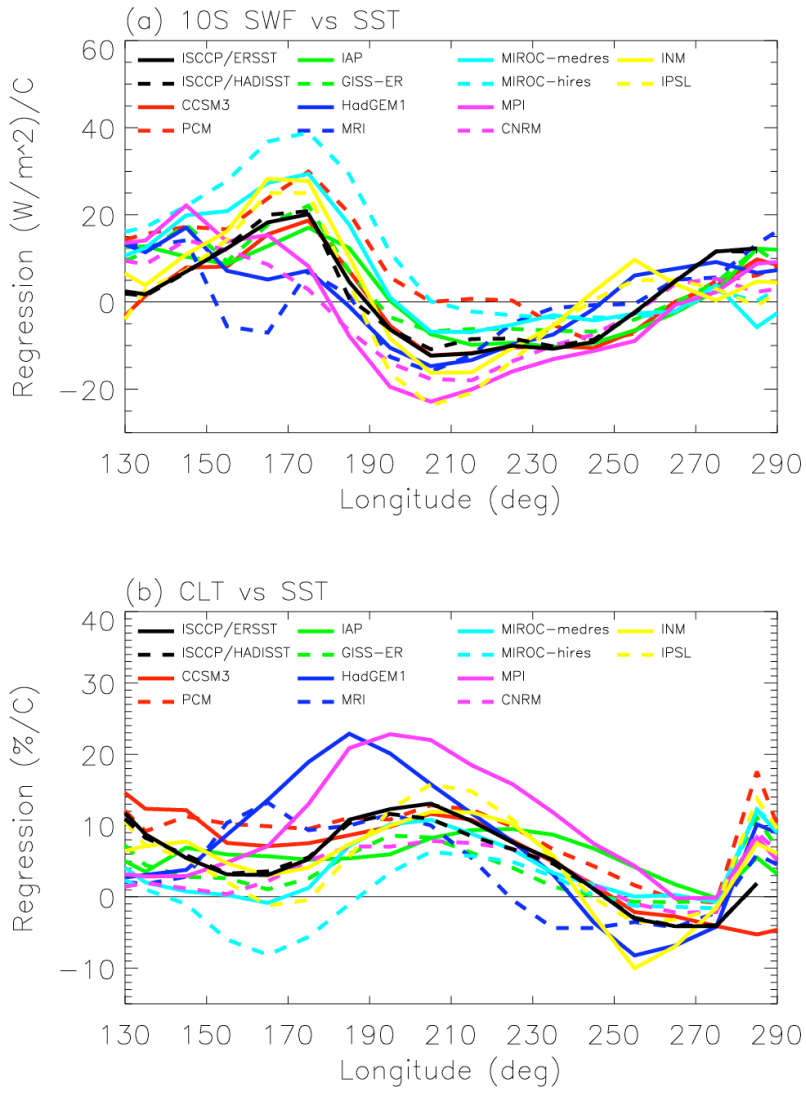

Figure 22. Same as Figure 16 but for 5S-15S averaged (a) SWF vs SST, and (b) total cloud amount vs SST.

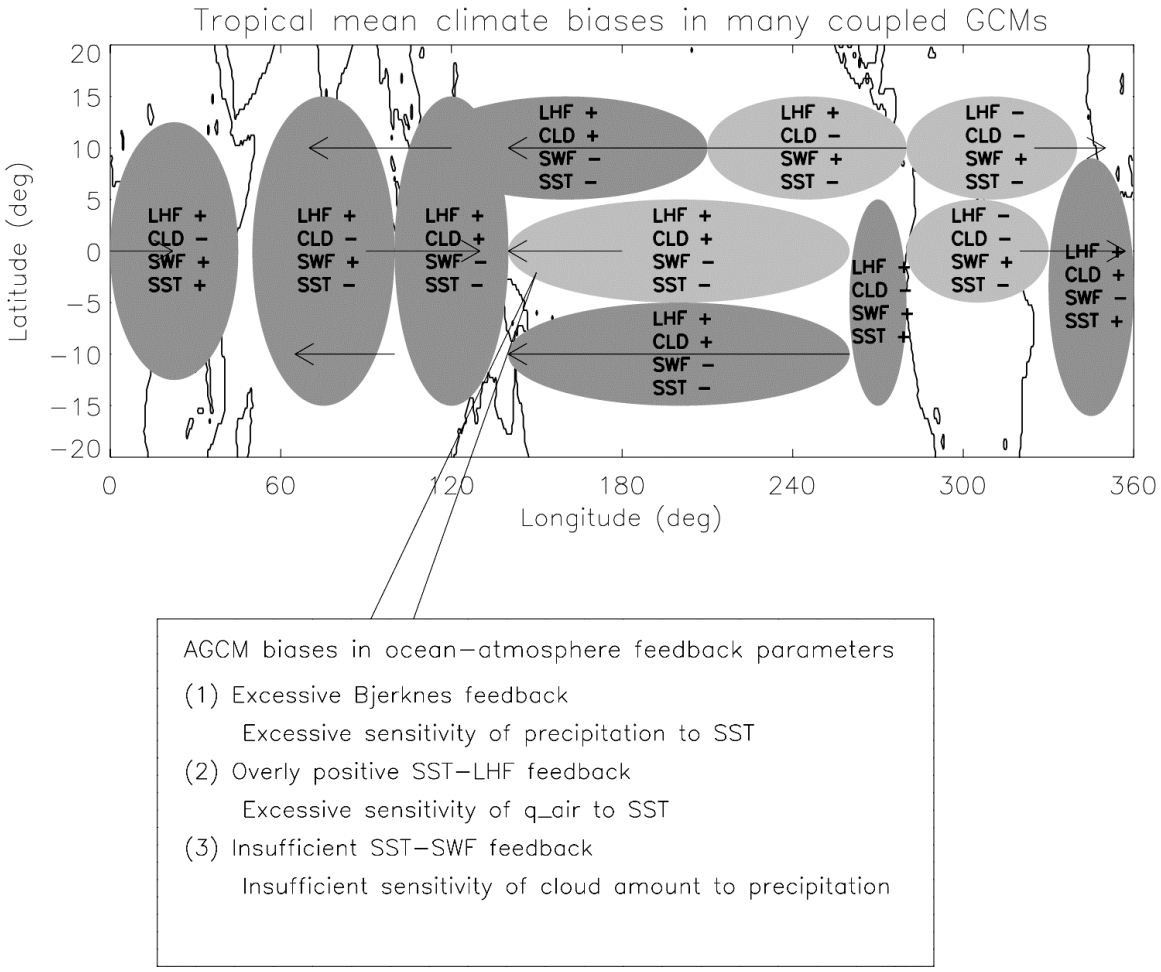

Figure 23. Schematic depiction of the tropical mean climate biases in many IPCC AR4 CGCMs. Dark shading denotes excessive precipitation, while light shading denotes insufficient precipitation. Arrow denotes surface zonal wind stress bias. The biases in total cloud amount (CLD), surface downward shortwave flux (SWF), surface latent heat flux (LHF), and SST are denoted by "+" for positive bias, and "-" for negative bias.